

**Compositing Digital Satellite Data to Detect Regions of  
Orographically Induced Convection on the Northern High Plains**

by  
Marjorie A. Klitch and Thomas H. Vonder Haar

Department of Atmospheric Science  
Colorado State University  
Fort Collins, Colorado



**Department of  
Atmospheric Science**

Paper No. 351

COMPOSITING DIGITAL SATELLITE DATA TO DETECT REGIONS  
OF OROGRAPHICALLY INDUCED CONVECTION ON THE NORTHERN HIGH PLAINS

Marjorie A. Klitch and Thomas H. Vonder Haar

Department of Atmospheric Science  
Colorado State University  
Fort Collins, CO 80523

July 1982

Atmospheric Science Paper No. 351

## ACKNOWLEDGEMENTS

Many individuals provided valuable support during the course of my research at Colorado State University. For their suggestions and advice I wish to thank my committee members, Dr. William Gray, Dr. Thomas Brubaker, and Dr. Thomas Vonder Haar, my adviser. Jan Behunek contributed useful technical advice and assistance. I greatly appreciate the comments, suggestions, stimulating discussions and helpful resources offered by Philip Durkee throughout my course of study.

Deep thanks are extended to Kristine Randolph for her expert programming advice, to Andrea Adams for her excellent work in preparing the typescript, to Duayne Barnhart for his photographic work, and to Judith Sorbie for her valuable assistance in drafting the figures in this paper. I also wish to acknowledge the Bureau of Reclamation, which supported this research under contract #9-07-85-V0025, and the many helpful people in their office of Atmospheric Resources Management.

Finally I sincerely thank my husband, Timothy, who tolerated long working hours on nights and weekends, and gave his support and encouragement from start to finish.

TABLE OF CONTENTS

<u>Chapter</u>	<u>Page</u>
Abstract . . . . .	ii
Acknowledgements . . . . .	iv
Table of Contents . . . . .	v
List of Tables . . . . .	vi
List of Figures . . . . .	vii
I. Introduction . . . . .	1
II. Procedure . . . . .	7
III. Data Analysis . . . . .	15
A. Cloud Frequency versus Surface Elevation . . . . .	15
B. Topographic Regions with Consistently High Cloud Frequencies . . . . .	30
C. Temporal Variations . . . . .	31
1. Diurnal Variations . . . . .	31
2. Month-to-Month Variations . . . . .	37
3. Year-to-Year Variations . . . . .	56
IV. Interpreting Temporal Variations with Available Weather Data . . . . .	58
V. Previous Cloud Climatological Studies . . . . .	64
VI. Summary and Conclusions . . . . .	74
A. Qualitative Analysis . . . . .	74
B. Quantitative Analysis . . . . .	74
C. Conclusion . . . . .	76
D. Suggestions for Future Research . . . . .	76
E. Potential Applications . . . . .	77
Bibliography . . . . .	80
Appendix . . . . .	83

LIST OF TABLES

<u>Table</u>	<u>Page</u>
1 Correlation and Regression Statistics for Surface Elevation (X) Versus Cloud Frequency as Shown in Composites of 18 GMT Visible Imagery (Y). . . . .	28
2 Correlation and Regression Statistics for Surface Elevation (X) Versus Cloud Frequency as Shown in Composites of 18 GMT Visible Imagery (Y). . . . .	28
3 Correlation and Regression Statistics for Surface Elevations of 4000 Feet and Above (X) Versus Cloud Frequency (Y) as Shown in Averages of the 18 GMT Visible and Infrared Composite Imagery. . . . .	29
4 Average Surface Moisture at 12 GMT . . . . .	60
5 Ranking the Months by Moisture Availability. . . . .	61
6 Ranking the Months by Average Cloud Frequency in the Composite Imagery. . . . .	62

LIST OF FIGURES

<u>Figure</u>	<u>Page</u>
1 Schematic representation of mountain-plains circulation (from Dirks, 1969). . . . .	3
2 Location of convective "hot spots" along the lee slopes of the Colorado Rockies (from Henz, 1973). . . . .	4
3 Flowchart for program YNSORT. . . . .	10
4a Visible enhancement function. . . . .	16
4b Infrared enhancement function . . . . .	16
5 Topography of the northern High Plains. . . . .	17
6 Surface elevation versus average cloud frequency for the average of all the 18 GMT (11 AM, Local Time) visible composites. . . . .	19
7a Composite of <u>visible</u> imagery, 18 GMT (11 AM, Local Time) June 1979 . . . . .	20
7b Composite of <u>infrared</u> imagery, 18 GMT (11 AM, Local Time) July 1979 . . . . .	20
8a Composite of <u>visible</u> imagery, 22 GMT (3 PM, Local Time) June 1979. . . . .	21
8b Composite of <u>infrared</u> imagery, 22 GMT (3 PM, Local Time) June 1979 . . . . .	21
9a Composite of <u>visible</u> imagery, 18 GMT (11 AM, Local Time) July 1979 . . . . .	22
9b Composite of <u>infrared</u> imagery, 18 GMT (11 AM, Local Time) July 1979 . . . . .	22
10a Composite of <u>visible</u> imagery, 22 GMT (3 PM, Local Time) July 1979 . . . . .	23
10b Composite of <u>infrared</u> imagery, 22 GMT (3 PM, Local Time) July 1979 . . . . .	23
11a Composite of <u>visible</u> imagery, 18 GMT (11 AM, Local Time) June 1980 . . . . .	24

<u>Figure</u>	<u>Page</u>
11b Composite of <u>infrared</u> imagery, 18 GMT (11 AM, Local Time) June 1980 . . . . .	24
12a Composite of <u>visible</u> imagery, 22 GMT (3 PM, Local Time) June 1980 . . . . .	25
12b Composite of <u>infrared</u> imagery, 22 GMT (3 PM, Local Time) June 1980 . . . . .	25
13a Composite of <u>visible</u> imagery, 18 GMT (11 AM, Local Time) July 1980 . . . . .	26
13b Composite of <u>infrared</u> imagery, 18 GMT (11 AM, Local Time) July 1980 . . . . .	26
14a Composite of <u>visible</u> imagery, 22 GMT (3 PM, Local Time) July 1980 . . . . .	27
14b Composite of <u>infrared</u> imagery, 22 GMT (3 PM, Local Time) July 1980 . . . . .	27
15 Fraction of month cloudy versus frequency within box from visible composites for 18 and 22 GMT (11 AM and 3 PM, Local Time) June 1979 . . . . .	33
16 Fraction of month cloudy versus frequency within box from visible composites for 18 and 22 GMT (11 AM and 3 PM, Local Time) July 1979 . . . . .	33
17 Fraction of month cloudy versus frequency within box from visible composites for 18 and 22 GMT (11 AM and 3 PM, Local Time) June 1980 . . . . .	34
18 Fraction of month cloudy versus frequency within box from visible composites for 18 and 22 GMT (11 AM and 3 PM, Local Time) July 1980 . . . . .	34
19 Fraction of month cloudy versus frequency within box from infrared composites for 18 and 22 GMT (11 AM and 3 PM, Local Time) June 1979 . . . . .	35
20 Fraction of month cloudy versus frequency within box from infrared composites for 18 and 22 GMT (11 AM and 3 PM, Local Time) July 1979 . . . . .	35
21 Fraction of month cloudy versus frequency within box from infrared composites for 18 and 22 GMT (11 AM and 3 PM, Local Time) June 1980 . . . . .	36
22 Fraction of month cloudy versus frequency within box from infrared composites for 18 and 22 GMT (11 AM and 3 PM, Local Time) July 1980 . . . . .	36

<u>Figure</u>	<u>Page</u>
23 Fraction of month cloudy versus frequency within quadrant for 18 GMT, June 1979 visible composite . . . . .	39
24 Fraction of month cloudy versus frequency within quadrant for 22 GMT, June 1979 visible composite . . . . .	40
25 Fraction of month cloudy versus frequency within quadrant for 18 GMT, July 1979 visible composite . . . . .	41
26 Fraction of month cloudy versus frequency within quadrant for 22 GMT, July 1979 visible composite . . . . .	42
27 Fraction of month cloudy versus frequency within quadrant for 18 GMT, June 1980 visible composite . . . . .	43
28 Fraction of month cloudy versus frequency within quadrant for 22 GMT, June 1980 visible composite . . . . .	44
29 Fraction of month cloudy versus frequency within quadrant for 18 GMT, July 1980 visible composite . . . . .	45
30 Fraction of month cloudy versus frequency within quadrant for 22 GMT, July 1980 visible composite . . . . .	46
31 Fraction of month cloudy versus frequency within quadrant for 18 GMT, June 1979 infrared composite. . . . .	47
32 Fraction of month cloudy versus frequency within quadrant for 22 GMT, June 1979 infrared composite. . . . .	48
33 Fraction of month cloudy versus frequency within quadrant for 18 GMT, July 1979 infrared composite. . . . .	49
34 Fraction of month cloudy versus frequency within quadrant for 22 GMT, July 1979 infrared composite. . . . .	50
35 Fraction of month cloudy versus frequency within quadrant for 18 GMT, June 1980 infrared composite. . . . .	51
36 Fraction of month cloudy versus frequency within quadrant for 22 GMT, June 1980 infrared composite. . . . .	52
37 Fraction of month cloudy versus frequency within quadrant for 18 GMT, July 1980 infrared composite. . . . .	53
38 Fraction of month cloudy versus frequency within quadrant for 22 GMT, July 1980 infrared composite. . . . .	54
39a Cloud count within the Miles City target site shown as percentages of the box with the highest count, box 3, 4 (from Reynolds and Vonder Haar, 1975) . . . . .	65

<u>Figure</u>	<u>Page</u>
39b Relative cloud count within the Miles City target site averaged by quadrants. . . . .	65
40a Average cloud frequency by quadrant for the average of the 18 GMT visible composites. . . . .	67
40b Average cloud frequency by quadrant for the average of the 18 GMT infrared composites . . . . .	67
41 Area for which the 1976 HIPLEX cloud climatology results are summarized (from Reynolds and Vonder Haar, 1978) . . . .	68
42 Number of clouds (per observation) versus time of day for the northern high plains for 1976 (from Reynolds and Vonder Haar, 1978). . . . .	69
43 Number of clouds (per observation) versus time of day for the Miles City target region for 1976 (from Reynolds and Vonder Haar, 1978) . . . . .	69

## I. INTRODUCTION

With the advent of spring and summer, regional and local influences on synoptic weather patterns become more pronounced. In mid-latitudes localized mesoscale convection generally dominates over synoptic controls, making forecasting a special challenge, particularly for those unfamiliar with local climatology. Topography directly affects the development of convective storms, especially along the lee slopes of the Rocky Mountains and the adjacent High Plains, where water resources command a high price due to the dry climate. Yet the High Plains along the eastern slopes of the Rockies serve as a major source region for summer severe weather events in the central United States (Miller, 1972). Convective storms form during the day and move, on the average, from west to east, resulting in frequent nighttime thunderstorms in the midwest. Indeed, Maddox (1980) noted that "small scale effects, such as topography and localized heat sources, may play important roles in initial storm development." He showed that almost half of the Mesoscale Convective Complexes (MCCs) documented in his study of 1978 Geostationary Operational Environmental Satellite (GOES) imagery, originated from thunderstorm activity initiated along the eastern slopes of the Rocky Mountains eventually organizing into massive systems that are largely responsible for the nocturnal maxima in thunderstorm frequency and precipitation over the central United States.

Convection is enhanced, if not caused, by surface heating which induces an unstable density stratification -- warmer, less dense air

below a cooler, denser layer --- that supports upward motion. Warm air, having the potential to hold more moisture than cool air, can release this moisture and expend latent heat energy when convection causes it to rise to the point where the moisture can condense, aggregate, and fall. Thunderstorms tend to move toward lower pressure and higher temperatures (Miller, 1972), so it might seem anomalous for convection to progress from west to east when the sun's heating marches from east to west. Yet the mountains and their gently sloping foothills receive their strongest insolation before local noon; the steeper the eastern aspect, the earlier the peak insolation. The influence of the mountains, then, is as if a solar heating impulse were moving from west to east, inducing upward motion as it goes.

Dirks (1969) included the effect of a slightly sloping plain in a numerical model of a large scale mountain-plain circulation. Strong descent in the immediate lee of the mountain and weak ascent of the broad region 100 to 300 km downwind characterized the two cell circulation (Fig. 1). Dirks noted that this circulation model could, with slight modifications, be applied to many areas around the world.

Phillip (1979) did a climatological study of two summers' satellite imagery observing convective interactions between the eastern slopes of the Colorado Rockies and the plains of eastern Colorado and western Kansas. Although the portion of precipitation in western Kansas and eastern Colorado attributable to mountain-to-plains systems varied somewhat from station to station, "satellite-identified days of development and movement contributed as much as 87% of a monthly total and 50% of the seasonal total precipitation" (Phillip, 1979). A significant portion of summer precipitation for stations in western Kansas could be

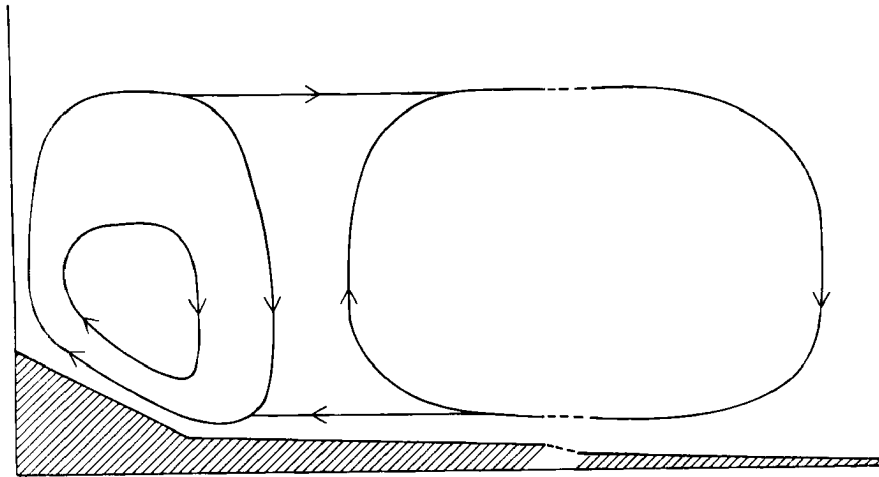


Fig. 1. Schematic representation of mountain-plains circulation (from Dirks, 1969).

attributed to convective activity that originated in the Colorado Rockies.

The mountain topography, of course, is more complex than that in Dirks' simple schematic, and so is the ensuing enhanced convection. Rather than a north-south convective line inferred from Dirks' two-dimensional diagram, convection seems to break out in preferred spots along the eastern slopes of the Rockies and western High Plains. With concern for severe convective storms that occur in Colorado, Henz (1973) used two summers of radar data and several types of severe storm information to determine "hot spots", which he defined as "regions of intense radar echo origin related to specific orographic or semi-permanent synoptic features which stimulate enhanced thunderstorm development." Henz's study examined those areas in Colorado observable from the National Weather Service (NWS) WSR-57 radar site near Limon, Colorado. Ten "hot spots", with an average size of about 200 sq. miles, along the eastern Colorado Rockies were identified (Fig. 2).

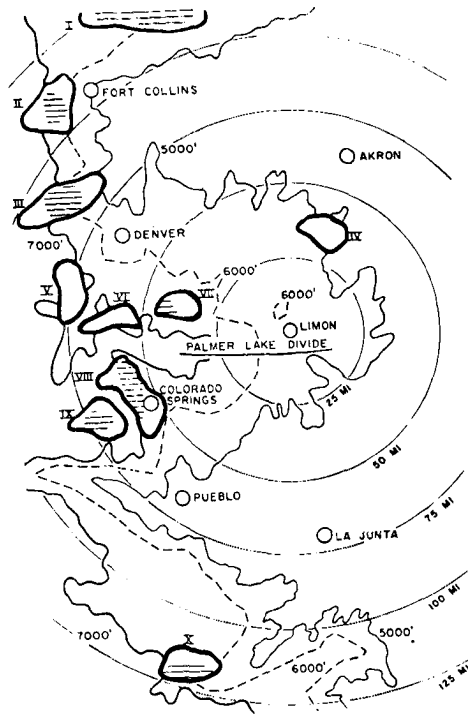


Fig. 2. Location of convective "hot spots" along the lee slopes of the Colorado Rockies (from Henz, 1973).

Seventy-three percent of all severe weather Henz observed during the 1970-1972 seasons was produced by "hot spot" originated convective systems, and 87% of all observed severe weather convective systems originated in the mountain-foothills complex. In addition, Henz noted that, on none of the days over the two years of study did all ten "hot spots" develop convective systems. He suggested that the limited amount of plains moisture may be funneled into the foothills complex by a mountain-valley breeze. The "hot spot envelope" for a particular month was elongated in the direction of the mid-level winds. His research supports the hypothesis, addressed by Grant (1974), that the mountains have a profound -- and somewhat predictable -- influence on summertime convection.

Radar echoes locate precipitating clouds by measuring the reflectivity, azimuth, and return time of pulsed signals. Realizing this, Klitch (1981) proposed that spots where topography enhances convective development (similar to Henz's "hot spots") could be detected using GOES imagery, which can locate clouds via visible light sensors and provide cloud top temperature information with infrared sensors. Focussing on the Montana Rockies, the convective source region for the HIPLEX/CCOPE<sup>1</sup> project, she averaged the visible imagery from four consecutive days in June 1980 at 18, 20, and 22 GMT and found eight suspected regions where topography enhances convective development -- tagged "suspected" because four days were not a large enough data sample to define these regions with great certainty. Nevertheless, the potential of compositing satellite imagery to locate areas where convection is more frequent was demonstrated and the influence of certain mountain ranges on convection in the northern High Plains was observed.

As is often the case, the early research on this problem prompted more questions than it answered. If compositing four days' satellite imagery could not conclusively identify regions where topography enhances convective development, would compositing an entire month's imagery work? If mid-level flow and availability of surface moisture determine whether or not a topographic feature induces convection on a particular day (as many supposed), how might one month's average compare to the next month's -- when normal long wave flow patterns may change?

---

<sup>1</sup>High Plains Experiment (HIPLEX) -- supervised by the Bureau of Reclamation under the Department of the Interior. The experiment site at Miles City, Montana was used for the Cooperative Convective Precipitation Experiment (CCOPE) in summer 1981.

How would the composites from one summer, say a typical-to-wet year (like 1979), compare to another (such as the anomalously dry summer of 1980)? Would these influential topographic features still show up? Would they be fainter, smaller in area, or present at all in the drought year? These questions, in turn, prompted this thesis research.

This paper strives to further refine the compositing technique in order to:

- a) more conclusively identify regions along the lee of the Montana Rockies where topography enhances convection, and
- b) explore the above questions on variability by comparing composite satellite imagery from consecutive summer months during two strikingly different consecutive summer seasons -- 1979 and 1980.

## II. PROCEDURE

The data used in this study were collected from the SMS-2 (GOES East) satellite by the Colorado State University Department of Atmospheric Science's Direct Readout Satellite Earth Station in Fort Collins, Colorado, for the HIPLEX project during summer 1979 and 1980. All data were received and recorded in digital form. Visible data were archived at one mile resolution;<sup>2</sup> the corresponding infrared data were archived at 4 by 2 mile resolution. Visible and infrared imagery was routinely recorded every half hour from 18 GMT to 01 GMT.<sup>3</sup> For Miles City, this is 12 noon to 7 p.m. local daylight time.

Before the data could be composited they had to be retrieved from the archive tapes, checked visually for errors in navigation or in archival, and stored so that imagery to be averaged together were all on one tape. The advantage of using GOES digital data over satellite photographs (e.g., Kornfield and Hasler, 1969) is that processing of digital data can be computer automated; also, more quantitative information can be extracted from digital data, such as energy fluxes, average brightness temperatures, and albedoes. Furthermore, analyzing satellite photographs can be confounded by variations in film density

---

<sup>2</sup>One pixel, or picture element, at satellite subpoint, approximately 75°W longitude, 0° latitude, measures one square mile.

<sup>3</sup>During 1979, data were not archived on Sundays.

and exposure that cannot be simply corrected by digitizing the photographs. The data were displayed on the 512 by 512 pixel ADVISAR-II/COMTAL Vision One-20 imaging system<sup>4</sup> in satellite coordinates centered at 46.42083°N, 105.89167°W (the location of Miles City) with a resolution of 0.02064:0.02530 (x:y) degrees per pixel. This resolution was chosen because it corresponds to the approximate resolution of the GOES-East data at Miles City. After the displayed images were visually checked, they were transferred to tape as 512 by 512 arrays, using the same center and resolution as above, so they could be composited. Eight tapes were prepared: 18 GMT Visible (June and July) 1980, 18 GMT Infrared 1980, 22 GMT Visible 1980, 22 GMT Infrared 1980, 18 GMT Visible 1979, 18 GMT Infrared 1979, 22 GMT Visible 1979, and 22 GMT Infrared 1979. It was discovered early in the research that the simple pixel by pixel averaging technique used earlier by Klitch (1981) would not be satisfactory because of "ground contamination." That is, the radiative characteristics of the ground would bias the average. Where the ground is dark, the Black Hills for example, the resulting average of visible data would be darker than for an area where the ground is light, such as the sandy Badlands, even with the same cloud frequency and cloud brightness characteristics. In the infrared ground contamination would not be as great as in the visible, but because infrared emissivities vary with soil type, the average infrared brightness could be biased by

---

<sup>4</sup>For a description of Colorado State University's Direct Readout Satellite Earth Station, which includes the ADVISAR II, see Klitch, 1982.

the different soils and vegetation over the region.<sup>5</sup> Because convective clouds are of interest here, two computer programs were created that selectively filter out the ground by ignoring values below a specified brightness threshold.

One program, called YNSORT (for Yes/No Sort), counts the frequency of brightnesses above the specified threshold at each pixel. The resultant 512 by 512 array can be displayed on the Colorado State University Department of Atmospheric Science's ADVISAR II. The program also adjusts the frequency values determined by YNSORT so that a value of zero represents a zero frequency of the images in the sample having a brightness above the cloud threshold. A value of 255 (the maximum input brightness count for the COMTAL image planes) corresponds to 100% of the images processed having brightnesses above the cloud threshold at that pixel. The composite image created by YNSORT is a mosaic of grey shades with the darkest areas having the lowest (or zero) frequency of clouds. Although similar to an average, the composite image depicts the frequency of cloud at each pixel. Figure 3 is a flow chart listing the major steps in the program YNSORT. Figures 9a and 14b are image output from YNSORT.

The program YNSORT yields quantitative information about the frequency of clouds over the area of study. As its name implies, it is a

---

<sup>5</sup>Certainly the relative differences in ground brightness, which can be expressed in terms of albedo, have meteorological importance. In fact differences in ground albedo can cause updrafts, commonly called "thermals," because the differential heating induces the warmer air to rise. Such updrafts promote mixing in the boundary layer and are of interest to other scientists. Nevertheless in examining the topographical influences on convective development, the bias ground albedo will introduce in cloud brightness calculations must be eliminated.

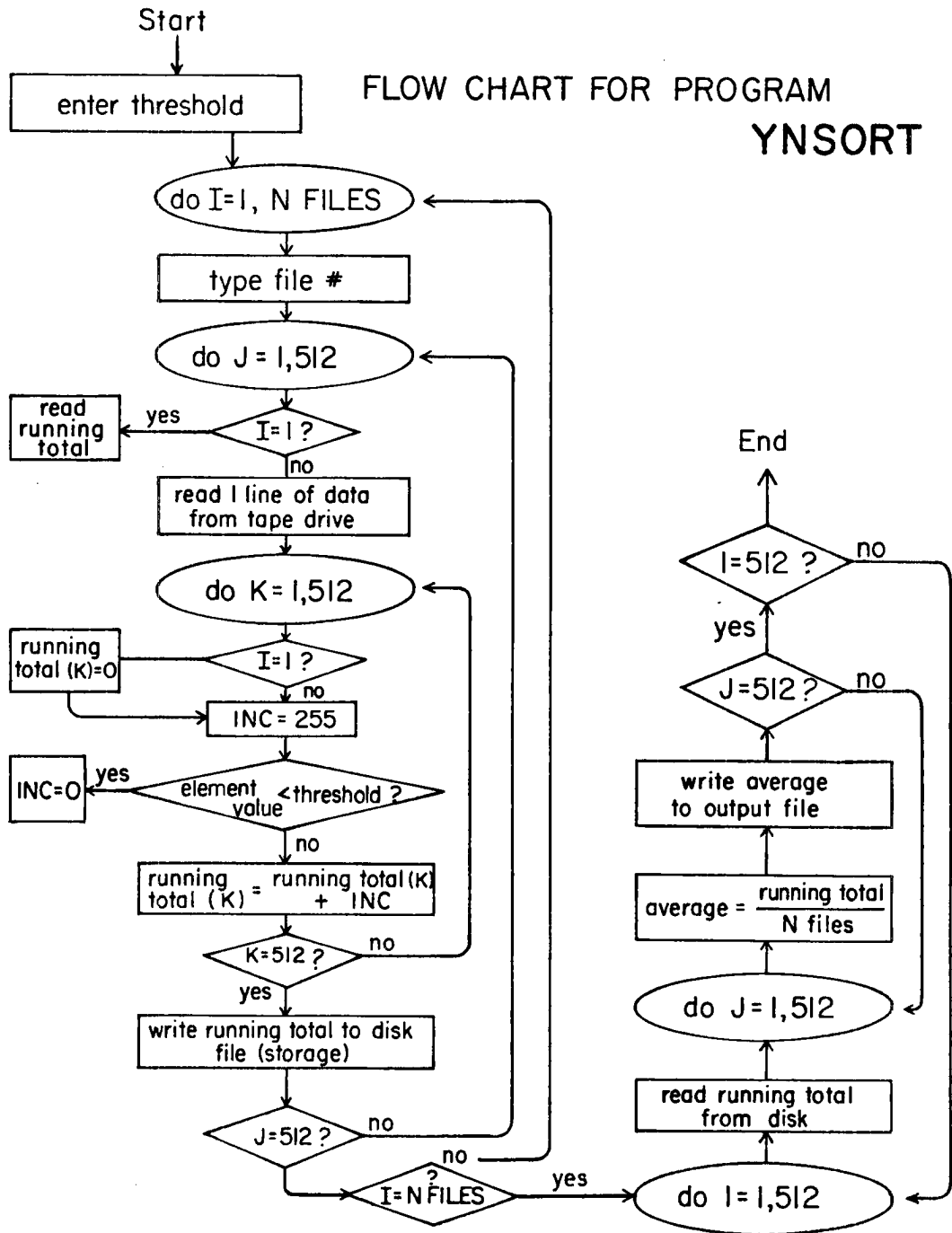


Fig. 3. Flowchart for program YNSORT.

computer automated Yes/No sort, which yields little information about the brightness of the clouds. Cloud brightness is also important because the visibly brightest clouds generally are the densest and deepest (Reynolds and Vonder Haar, 1973). Infrared brightness corresponds to temperature: the brightest clouds in the infrared also have the coldest tops. Infrared brightness indicates the extent of vertical development (until the cloud tops reach the tropopause)<sup>6</sup> and potential for intense releases of latent heat energy -- hail, tornadoes, heavy rain, and high winds. A separate program, called BRTAVG, was written to enable the computation of average cloud-only brightness for each pixel, while still eliminating the bias of ground contamination. Statistical and computational problems arose in attempting to process image data in this manner on the ADVISAR II's PDP 11/60 minicomputer. Computing the average cloud-only brightness requires storage of additional 512 by 512 arrays and, as a result, quadruples the I/O (input/output) of an already I/O bound program.<sup>7</sup>

Statistical complications in determining the average "cloud only" brightness at each pixel, arise due to the fact that the frequency of clouds varies at each pixel. In comparing averages, as is done in scrutinizing a composite image, one must consider the statistical significance of each average, as it determines the average's reliability, or the confidence that can be placed in it. More confidence can be placed in an average brightness resulting from, say 15 images (or about

---

<sup>6</sup>Above the tropopause, of course, temperature increases with height.

<sup>7</sup>Such computations will be entirely feasible and much more efficient when the ADVISAR II acquires a VAX 11/780 as its host computer.

50% of the sample) than in an average derived from only one or two in the sample with an average brightness above the cloud threshold. Because of these two complications, analyzing the visible and infrared brightness information to indicate where the brighter (implying deeper) clouds tend to form by computing an average cloud-only brightness was postponed until the computational and statistical problems could be solved.

The program YNSORT was run on each of the 16 data sets. The cloud threshold used for the 18 GMT visible data was 28 (of a maximum 64 counts) and a count of 26 was the threshold for the 22 GMT visible data. The threshold for all infrared compositing was 154 (of a maximum 255 counts), which corresponds to an equivalent black body temperature of  $-20^{\circ}\text{C}$ . The resulting arrays were displayed on the ADVISAR II and the areas with the highest cloud frequencies were located. Then a pixel brightness frequency counting routine, called PIXCNT, was run on each composite. PIXCNT counts the number of pixels in a specified area having a given input count, or brightness, on a COMTAL image plane. The output from PIXCNT was input for a simple averaging program (run on the VAX 11/780) that computes the overall average count for the region and the relative frequency of all counts. The regions studied were a large box centered at Miles City with dimensions 256 by 256 pixels<sup>8</sup> and the four quadrants within this box, each 128 by 128 pixels in size. Statistics were compiled for the large box and for each quadrant and compared with one another as well as with earlier cloud statistics compiled for the HIPELX area (Reynolds and Vonder Haar, 1975; Reynolds and Vonder Haar, 1978; and Stodt, 1978).

---

<sup>8</sup>This corresponds to about 400 km E/W by 720 km N/S.

Next, the composites were displayed on the ADVISAR II and visually compared to observe the similarities and differences between the 1979 and 1980 seasons, the months of June and July, the hours of 18 and 22 GMT and between visible and infrared composite imagery. The bright spots common to pairs of composites were noted and their geographic locations determined. These coordinates were located on aeronautical charts. The approximate surface elevation for each point was recorded, along with its proximity to any mountain peaks, ridges, reservoirs, or riverbeds. A bright spot on a single composite could occur by chance; but if the same bright area is common to many pairs of composites, it is more likely a region where convective development is enhanced.

To demonstrate and quantify the relationship between surface topography and composite cloudiness, a plot of surface elevation versus composite brightness was constructed for each of the 18 GMT composites, as well as for an average of the four. Cloud frequencies, as indicated by the composite imagery, were read from the ADVISAR screen. The value of every 32nd pixel and its latitude and longitude were recorded, so that the corresponding surface elevation for each of these points could be retrieved. Surface elevation was estimated from aeronautical maps to within about 500 feet. After surface elevation was plotted against cloud frequency, a linear model was assumed and the correlation for the regression line was determined. A positive correlation coefficient close to one would indicate a strong, positive, linear correlation between surface elevation and cloud frequency -- that is, the higher the elevation, the greater the composite response. A correlation coefficient near zero would mean the data show little, or at best, a very sketchy, relationship between surface elevation and cloud frequency;

and a negative correlation coefficient close to negative one would indicate a strong negative correlation -- the higher the elevation, the more cloud-free the composite response.

### III. DATA ANALYSIS

Recall that the composites depict cloud frequency at a particular time of day over a month. To assist in interpretation of the composite imagery, a legend with COMTAL brightnesses from zero (black) to 255 (brightest white), and the cloud frequency each shade corresponds to, was displayed across the top of each image. Because a cold cloud threshold was used in compositing the infrared imagery, not all clouds detected in the visible were detected in the infrared. Therefore, the cloud frequencies in the infrared composites were generally lower than in their visible counterparts.\* To make the highest infrared cloud frequencies stand out, the infrared composites were displayed with an enhancement function that makes the lower frequencies appear brighter. This enhancement function, and the normal linear enhancement used for the visible composites are shown in Figs. 4a and 4b.

#### III.A Cloud Frequency Versus Surface Elevation

A cursory look at the composite imagery (Figs. 7a-14b) showed regions of high cloud frequency collocated with mountain peaks and ranges. The local topography of the northern High Plains is shown in Fig. 5. When surface elevation was plotted against cloud frequency at 18 GMT, a clear positive linear correlation between the two was expected. Figure 6 shows the plot of surface elevation versus cloud frequency for the average of all the 18 GMT visible composites. This

---

\*For a treatment of radiative theory pertinent to interpretation of the composite imagery see Klitch, 1982. Sources of error are discussed in the Appendix.

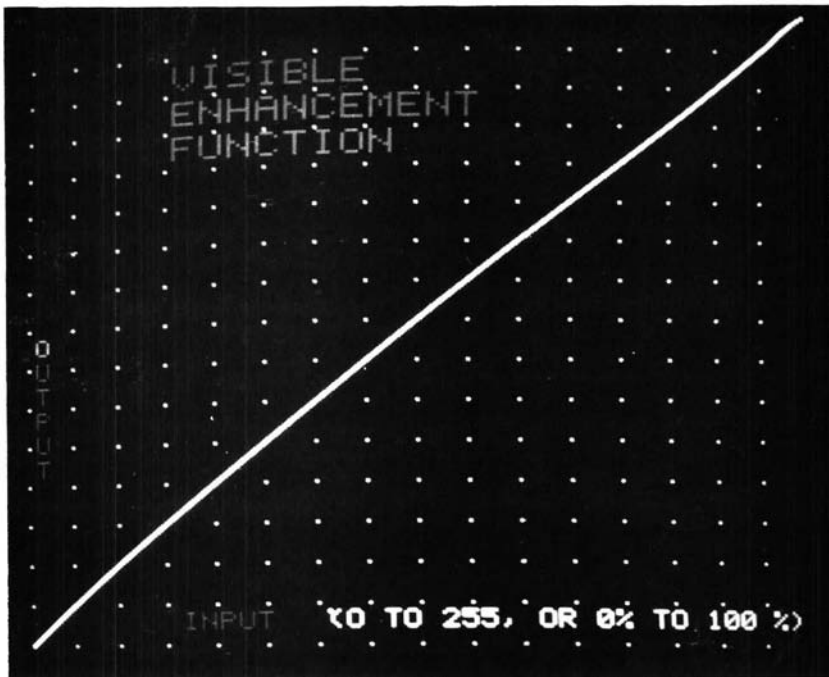


Figure 4a. Visible enhancement function.

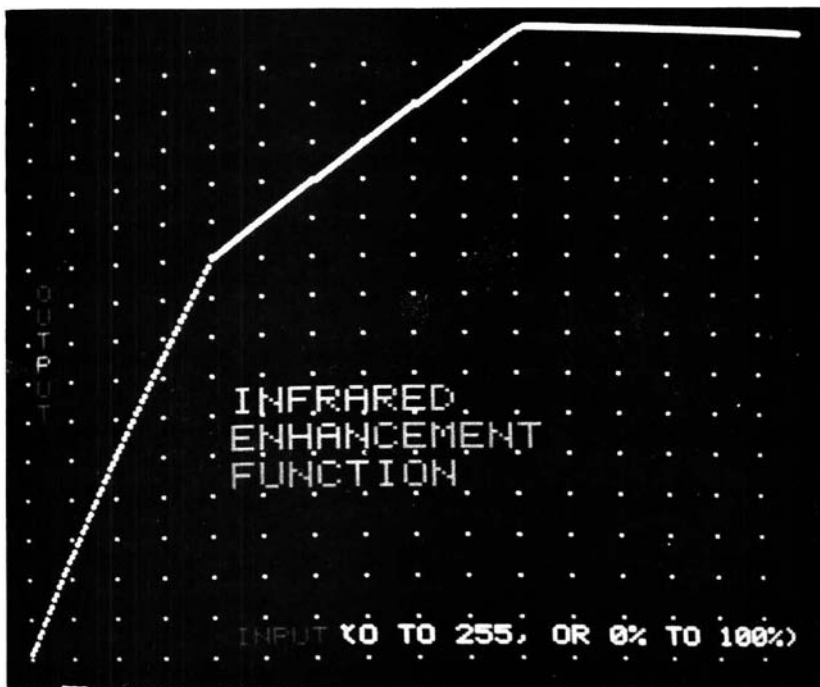


Figure 4b. Infrared enhancement function.



Fig. 5. Topography of the northern High Plains. Height contours are in meters above mean sea level.

plot shows, if anything, a negative relationship between surface elevation and cloud frequency when the whole area from the Rockies to the eastern Dakotas was sampled. This surprising result was suspected to be due to bias introduced by the July 1979 18 GMT composite (Fig. 9a). In this image, unlike the others, a higher incidence of cloudiness occurs east of the Montana border, where surface elevations are lower. Yet, the influence of the Big Horns, the Absarokas, and several other western mountains is apparent. Several reasons may account for the anomalously high cloud frequencies in the Dakotas, including:

- a) remnants of MCC's were present in that vicinity on several days; or
- b) a dry line, common at this same longitude in Texas, persisted approximately along the eastern Montana border during the month, effectively preventing much moisture from being available further west; or most likely
- c) the observations were made over too large an area, with too wide a range of elevations. When only elevations above 1500 meters are considered, a positive correlation between surface elevation and cloud frequency emerges.

Note, too, that the July 1979 18 GMT infrared composite indicates a higher frequency of clouds colder than  $-20^{\circ}\text{C}$  in the Dakotas (Fig. 9b). Similarly, the plot of surface elevation versus cloud frequency for the average of all 18 GMT infrared composites did not show any positive linear relationship.

To ascertain whether or not these averaged composites were indeed biased by the anomalous July 1979 composite, surface elevation versus composite response was plotted for each of the component 18 GMT composite images: June 1979, July 1979, June 1980, and July 1980. A program computing correlation and regression statistics was run, using

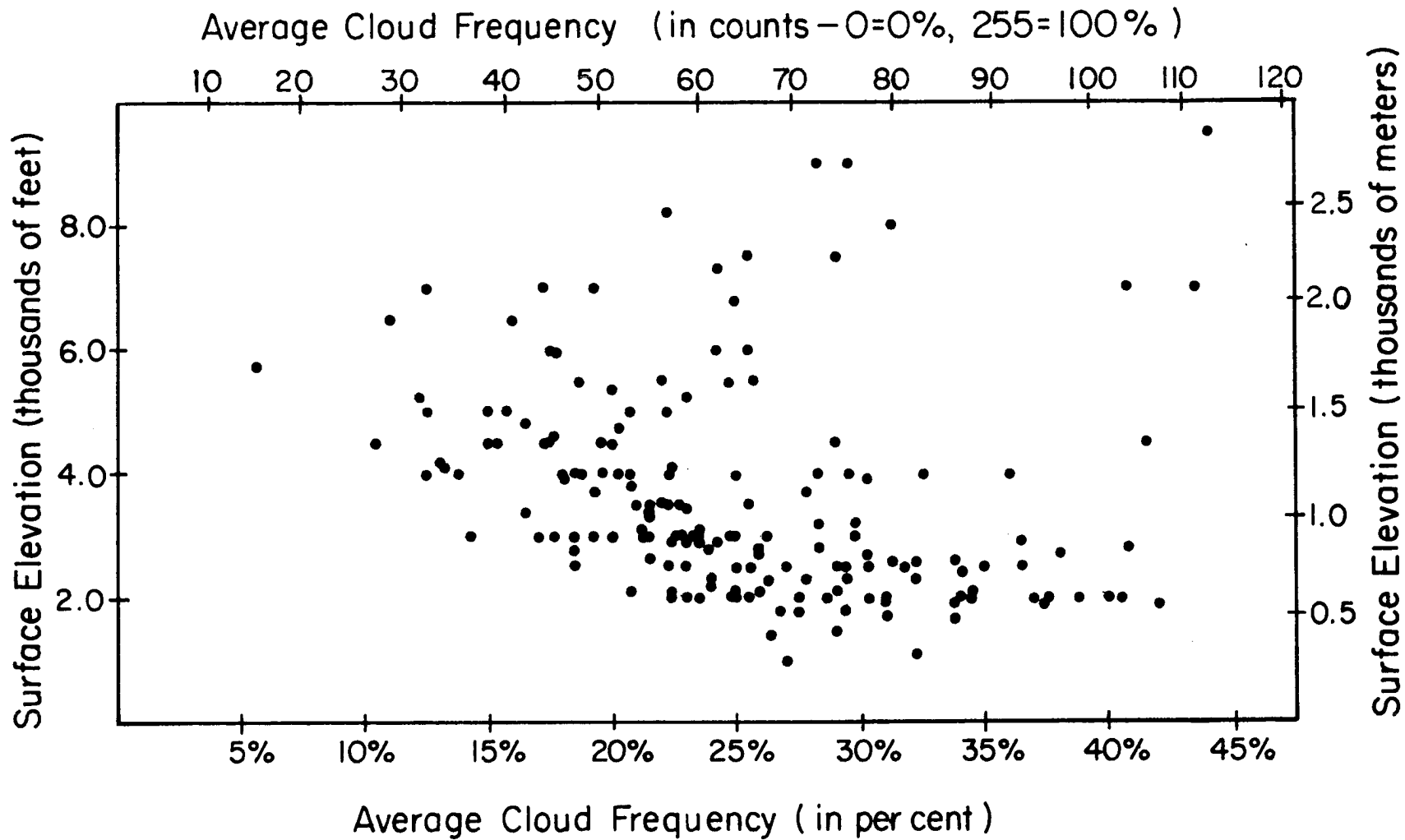


Fig. 6. Surface elevation versus average cloud frequency for the average of all the 18 GMT visible composites.

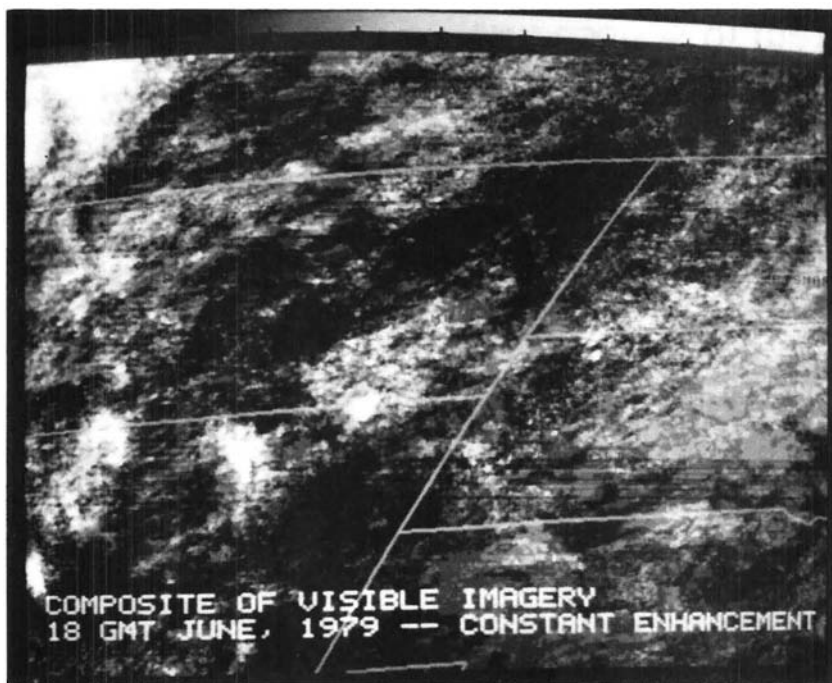


Figure 7a. Composite of visible imagery, 18 GMT (11 AM, Local Time) June 1979.

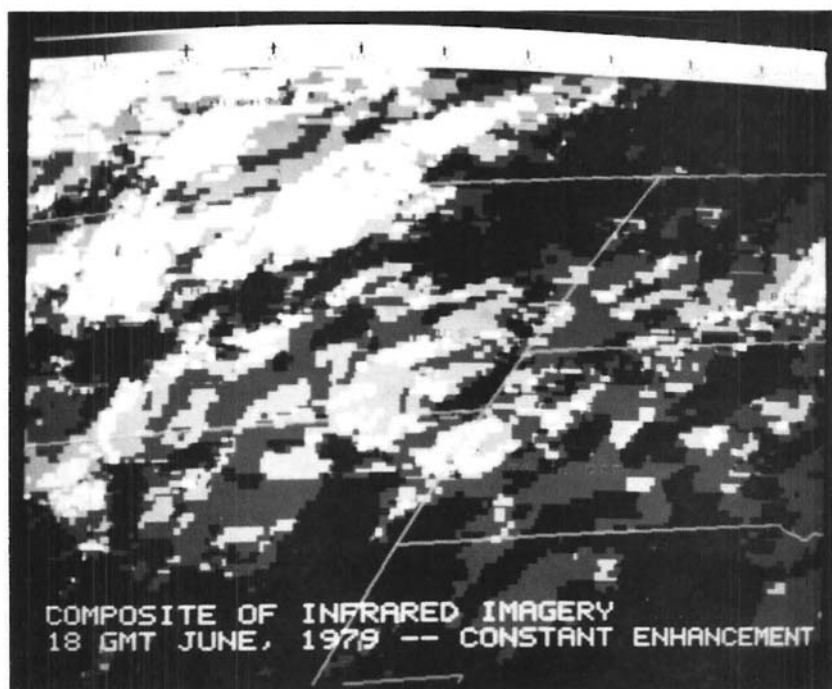


Figure 7b. Composite of infrared imagery, 18 GMT (11 AM, Local Time) June 1979.

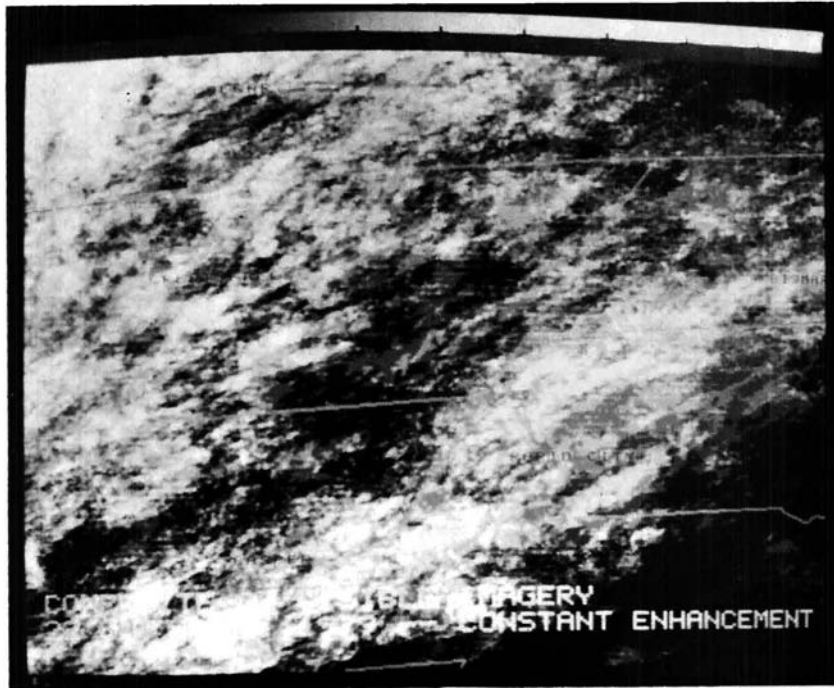


Figure 8a. Composite of visible imagery, 22 GMT (3 PM, Local Time) June 1979.

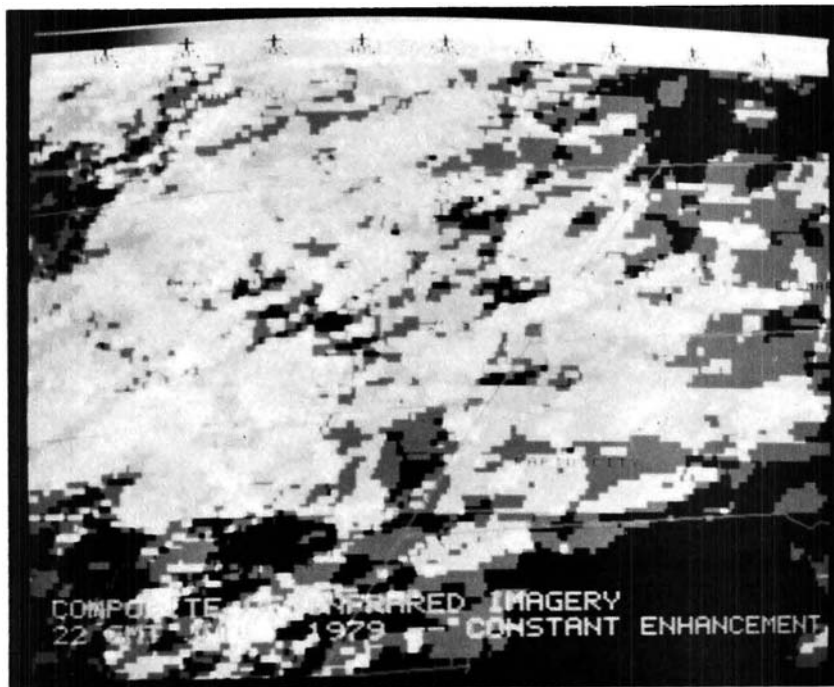


Figure 8b. Composite of infrared imagery, 22 GMT (3 PM, Local Time) June 1979.

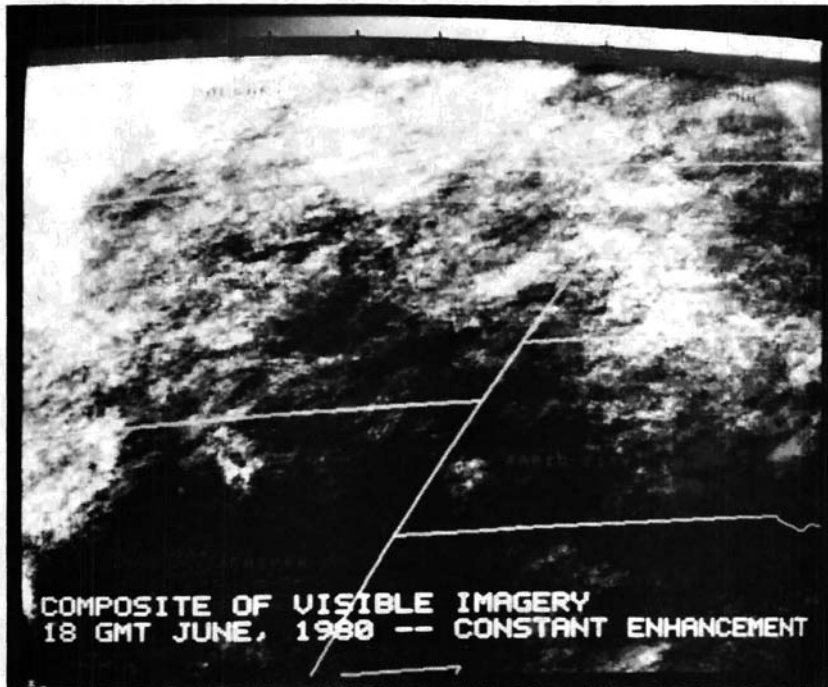


Figure 11a. Composite of visible imagery, 18 GMT (11 AM, Local Time) June 1980.

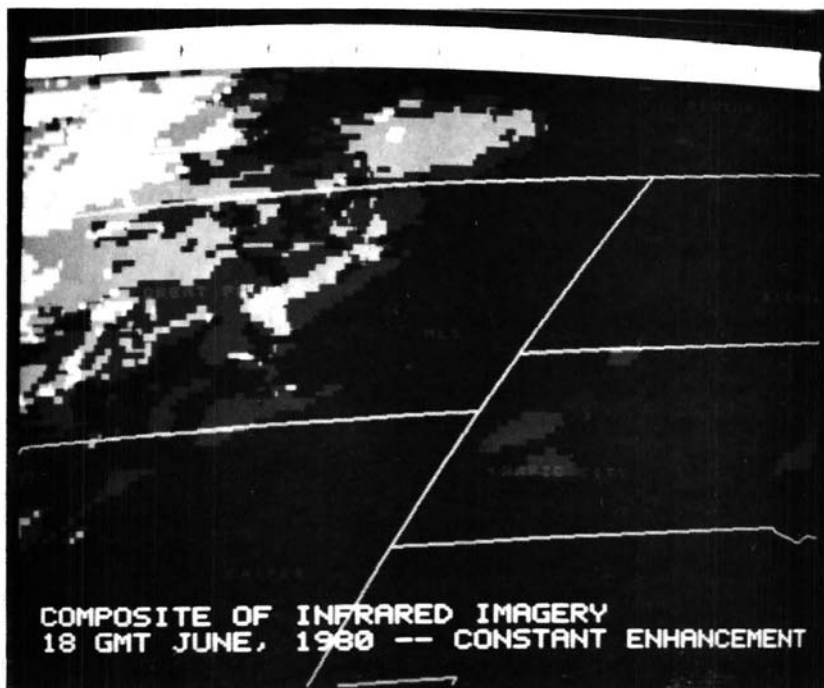


Figure 11b. Composite of infrared imagery, 18 GMT (11 AM, Local Time) June 1980.

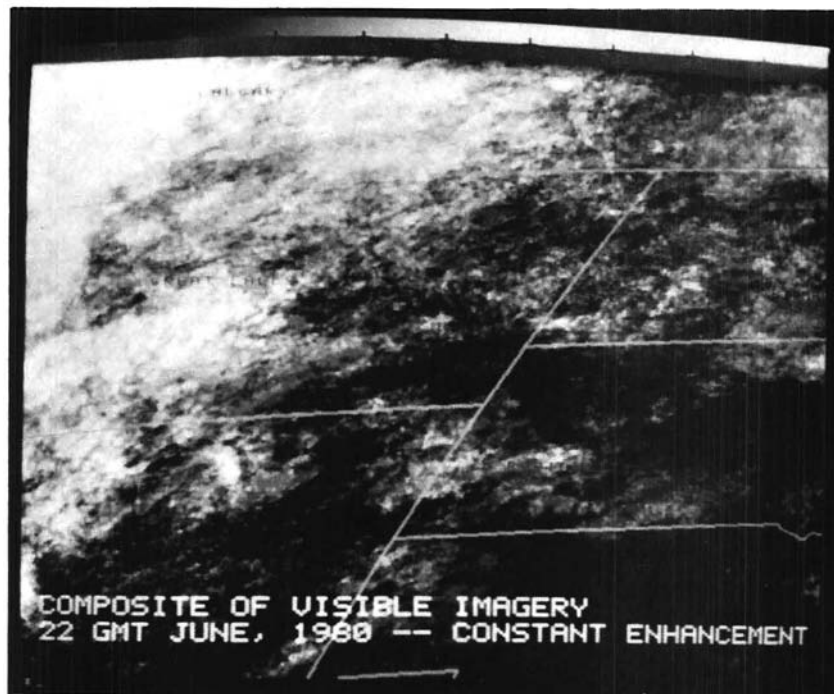


Figure 12a. Composite of visible imagery, 22 GMT (3 PM, Local Time) June 1980.

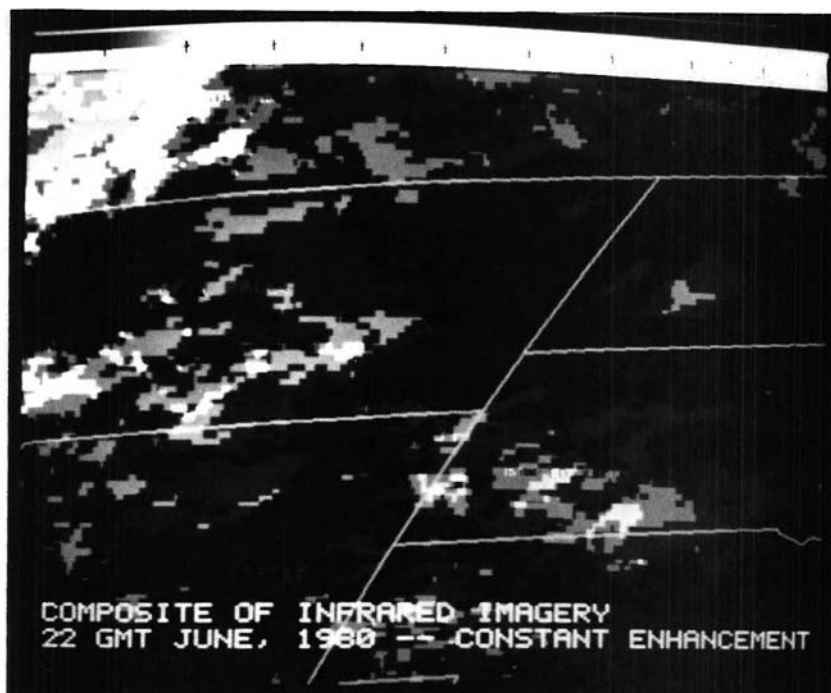


Figure 12b. Composite of infrared imagery, 22 GMT (3 PM, Local Time) June 1980.

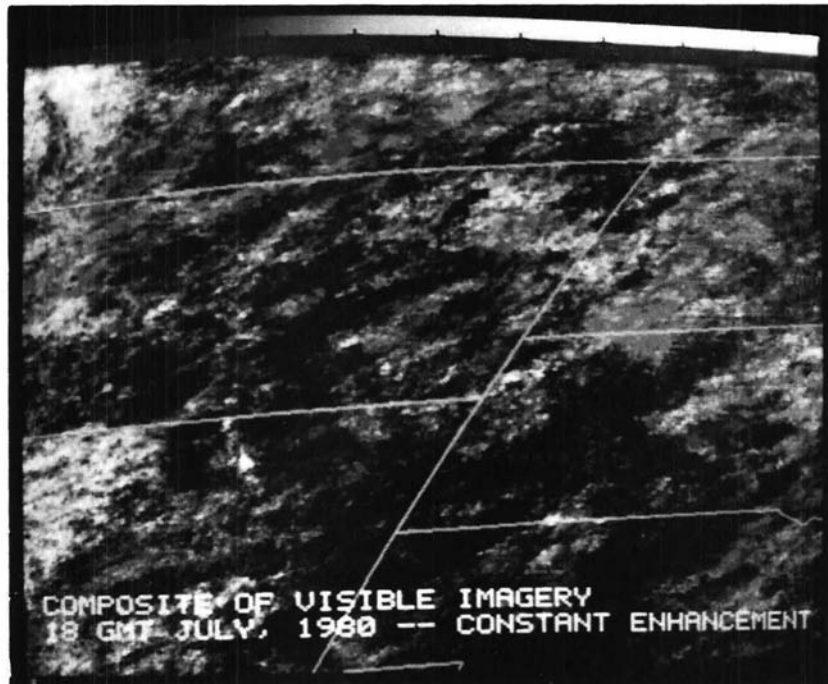


Figure 13a. Composite of visible imagery, 18 GMT (11 AM, Local Time) July 1980.

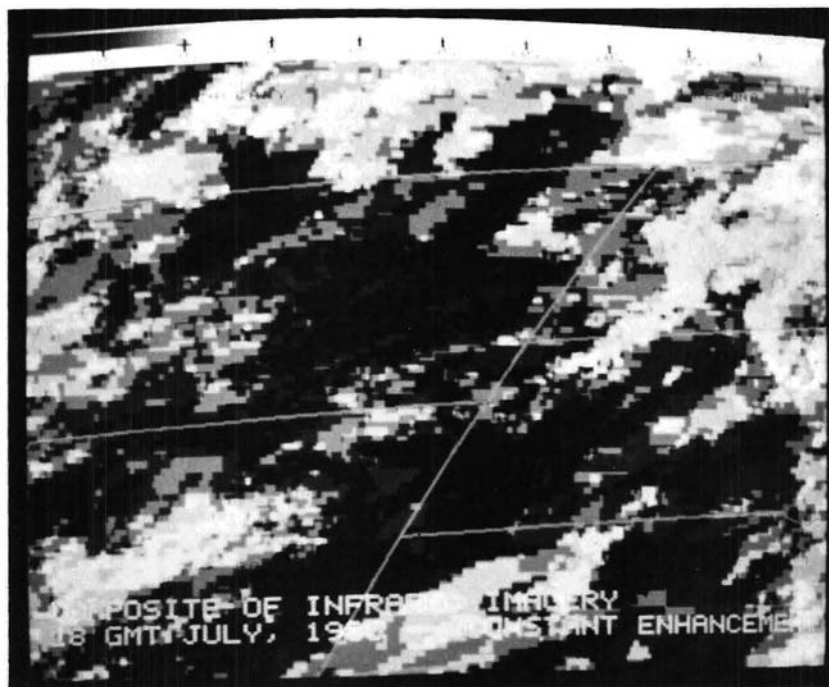


Figure 13b. Composite of infrared imagery, 18 GMT (11 AM, Local Time) July 1980.

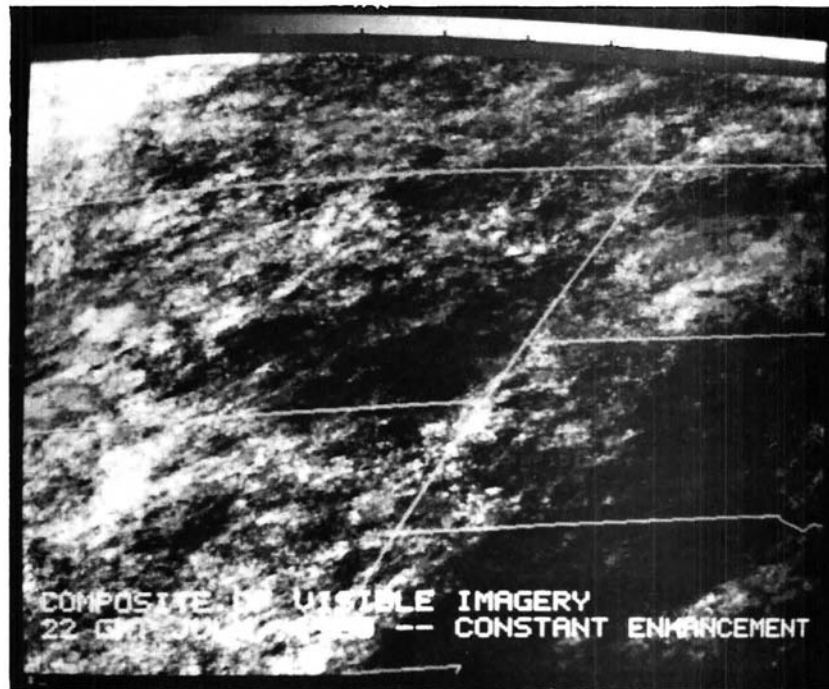


Figure 14a. Composite of visible imagery, 22 GMT (3 PM, Local Time) July 1980.

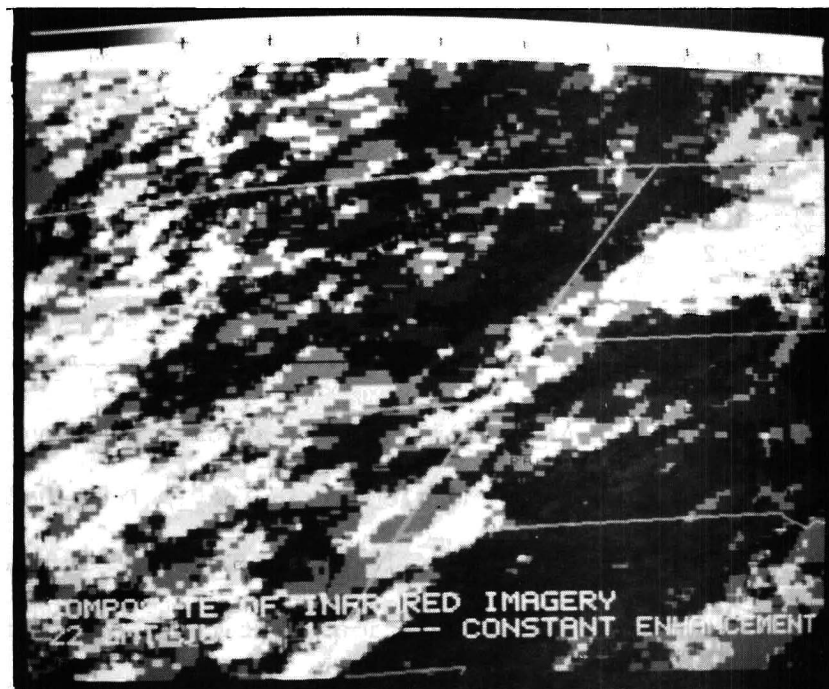


Figure 14b. Composite of infrared imagery, 22 GMT (3 PM, Local Time) July 1980.

the VAX 11/780, on all these data. The statistics are summarized below in Tables 1 and 2.

Table 1

Correlation and Regression Statistics for  
Surface Elevation (X) Versus Cloud Frequency as  
Shown in Composites of 18 GMT Visible Imagery (Y)

	Average Count	Equivalent % Frequency	Regression $\alpha$	$\beta$	$\sigma$	Correlation Coefficient
June 1979	68.7	26.96%	73.8	-.00141	563	-.100
July 1979	66.7	26.15%	98.1	-.00876	1122	-.402
June 1980	59.7	23.41%	65.4	-.00158	1091	-.080
July 1980	62.0	24.31%	60.0	+.00055	513	+.041
Average Composite	63.9	25.07%	74.0	-.00281	318	-.256

Table 2

Correlation and Regression Statistics for  
Surface Elevation (X) Versus Cloud Frequency as  
Shown in Composites of 18 GMT Visible Imagery (Y)

	Average Count	Equivalent % Frequency	Regression $\alpha$	$\beta$	$\sigma$	Correlation Coefficient
June 1979	26.0	9.79%	25.5	-.00015	319	-.014
July 1979	24.9	9.75%	40.7	-.00441	316	-.385
June 1980	8.2	3.23%	6.6	+.00046	116	+.071
July 1980	28.2	11.05%	30.7	-.00069	300	-.066
Average Composite	21.1	8.23%	25.5	-.00122	72	-.234

Individually, none of the plots heralded any strong, positive correlation between surface elevation and cloud frequency. Indeed, Tables 1 and 2 show that only one of the four 18 GMT visible and infrared composites exhibits any positive correlation. Yet the coefficient is so small that no substantial relationship can be implied, assuming a linear model. The bias of negative correlation in July 1979 composite is apparent, but still not really significant. Combining the other

three months would still not result in a strong positive correlation, as was originally expected.

It is important to note in Fig. 6 that when only elevations above 1500 meters are considered, a positive correlation between surface elevation and cloud frequency emerges. After this was observed, the correlation and regression program was run on the subset of observations with surface elevations of 4000 feet (approximately 1200 meters) and above. Table 3 shows these statistics. The positive correlation for the average visible composite is weak (.3507) and that for the average infrared composite is insignificant (.0379). [However these figures verify the positive correlation between cloud frequency and surface elevation above 1500 meters.] This relationship might appear stronger if surface elevation were estimated more accurately than to the nearest 500 feet and if factors such as parallax error and downwind formation of orographic clouds could be accounted for.

Table 3

Correlation and Regression Statistics for  
Surface Elevations of 4000 Feet and Above (X) Versus Cloud Frequency (Y),  
As Shown in Averages of the 18 GMT Visible and Infrared Composite Imagery

	Average Count	Equivalent % Frequency	Regression $\alpha$	$\beta$	$\sigma$	Correlation Coefficient
Average Visible Composite	55.1	21.6%	28.2	0.0050	379	.3507
Average Infrared Composite	18.1	7.1%	16.7	0.0003	106	.0379

From these results, surface elevation alone may not be the best index from which to infer topographical influences on convection across the northern High Plains. However, for elevations above 1500 meters it

is positively correlated with cloud frequency. The fact that most atmospheric moisture is contained in the lower layers of the atmosphere is one basic reason for the general aridity of the High Plains. And moisture is undeniably necessary for the formation of clouds. Stratifying the source imagery by environmental conditions, for example separating the data into an "enhanced" and a "suppressed" set, instead of by months might serve to show more of a mountain effect. The influence of mountains in the tropics, where moisture availability is not a problem, is well established. The above correlation and regression results support the hypothesis that not all mountains have the same effect. Qualitatively, the composites show that some mountains and elevated regions are positively correlated with cloud frequency, perhaps due to their eastern aspect and slope.

### III.B Topographic Regions with Consistently High Cloud Frequencies

A primary objective here is to identify the regions along the lee of the Montana Rockies where topography enhances convection. Although elevation does not seem to be correlated with cloud frequency on the broad scale, this primary objective can still be achieved.

Visually comparing the composites for common spots of high cloud frequency yielded several mountainous regions which repeatedly had a high cloud frequency. These regions are:

- 1) The Absarokas
- 2) The Big Horns
- 3) The Bear Paw Mountains (due south of Havre, Montana)
- 4) The Big Snowy Mountains (due south of Lewistown, Montana)
- 5) The ridgy area south and southwest of Miles City, Montana
- 6) The Canadian Rockies west of Calgary

With the exception of (5) and (6),<sup>9</sup> these mountains all are the most significant high spot within a radius of at least 50 km. The relief in the ridgy area south of Miles City (5) is more subtle, and the intensity of its influence on convection does not appear as great as that of the other regions listed above. Because these mountains are the most significant high spot within a radius of 50 km, they not only have a favorable eastern aspect for Dirks' mountain-plain circulation, but almost every wind direction will provide some upslope, making them more likely to induce convection than other topographic features.

### III.C Temporal Variations

A secondary objective of this research was to explore the temporal variability of the influence of these critical topographic regions on convection. Based on what is already known about the evolution of convection on the High Plains, hypotheses of the expected diurnal, month-to-month, and year-to-year variations in the composite imagery were formed before the composites were examined. In this section the observed variations in the composites will be discussed in light of the expected or hypothetical differences.

#### III.C.1 Diurnal Variations

Having observed and studied the evolution of summertime convection on the High Plains from the vantage of Fort Collins, Colorado, for several seasons, the author noted that convective clouds generally form over the mountains and foothills by mid-morning to noon, while the

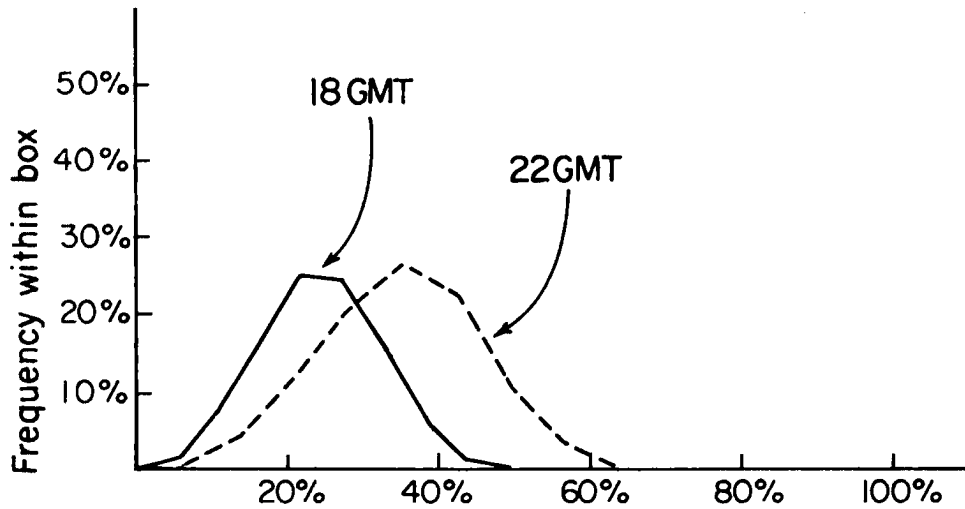
---

<sup>9</sup>Detailed topographic maps north of the United States border were not consulted.

adjacent High Plains remain relatively cloud-free. During the early afternoon convection spreads -- typically cumulus humilis or cumulus congestus are spread throughout the whole sky. From mid-afternoon until sunset, development of thunderstorms is usually observed, with activity generally peaking, and with the most severe events usually occurring, around 0 GMT (or 5 p.m. LST). Based on this scenario, the 18 GMT composites (11 a.m. LST) should show evidence of initial cumulus formation over the Montana mountains and foothills, with the adjacent High Plains mostly clear; whereas the 22 GMT composites (3 p.m. LST) should exhibit more widespread convection with deeper development just beginning. The 22 GMT composites ought to be generally brighter than the 18 GMT composites because of the more widespread cumulus development expected. Observations of both the visible and infrared composites seem to verify this hypothesis, with a few exceptions. In all the June composites, the 22 GMT imagery looks slightly brighter than the 18 GMT. However in the July composites only the 1979 infrared imagery shows more general cloudiness at 22 GMT. The other three July comparisons do not clearly show whether or not the 22 GMT composite has an overall higher frequency of cloudiness. Qualitatively the hypothesis that 22 GMT imagery ought to exhibit more overall cloudiness is verified for the June composites but the July imagery is neither sufficient to verify nor to deny this hypothesis.

Apart from visually comparing the composites for qualitative diurnal differences in overall cloud frequency, the results from PIXCNT can be objectively examined to quantitatively measure the differences between the 18 GMT and 22 GMT composites. Figs. 15-22 are plots showing the number of pixels with each resultant cloud frequency for 18 GMT and 22 GMT. While the spatial depiction of cloud frequency in Figs. 7a-14b

## Fraction of month cloudy     June 1979

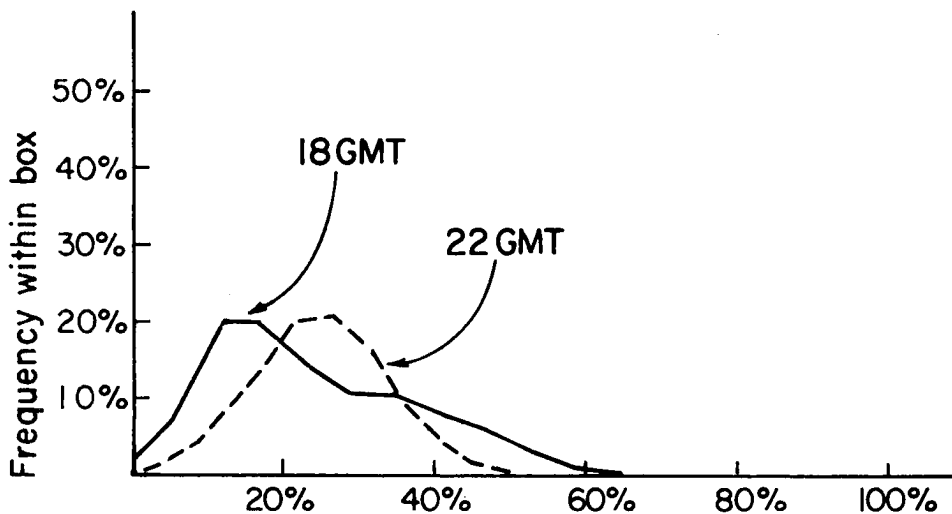


18 GMT Average Frequency = 25.0 %

22 GMT Average Frequency = 35.6 %

Fig. 15. Fraction of month cloudy versus frequency within box from visible composites for 18 and 22 GMT (11 AM and 3 PM, Local Time) June 1979. In this example, roughly 25% (the mode) of the pixels had a cloud frequency of about 22% at 18 GMT, whereas at 22 GMT the mode (again about 22% of the pixels) had a higher cloud frequency of about 35%.

## Fraction of month cloudy     July 1979

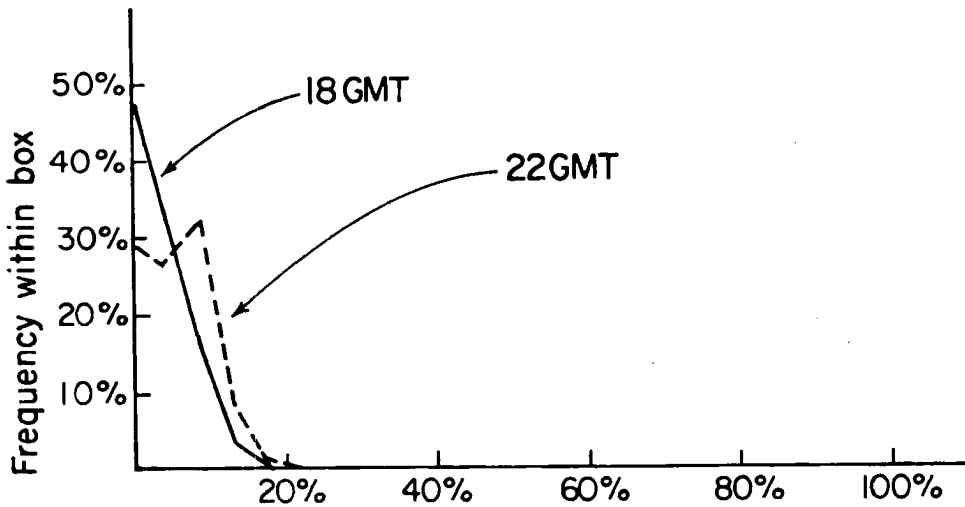


18 GMT Average Frequency = 24.3 %

22 GMT Average Frequency = 25.2 %

Fig. 16. Fraction of month cloudy versus frequency within box from visible composites for 18 and 22 GMT (11 AM and 3 PM, Local Time) July 1979.

Fraction of month cloudy      June 1980

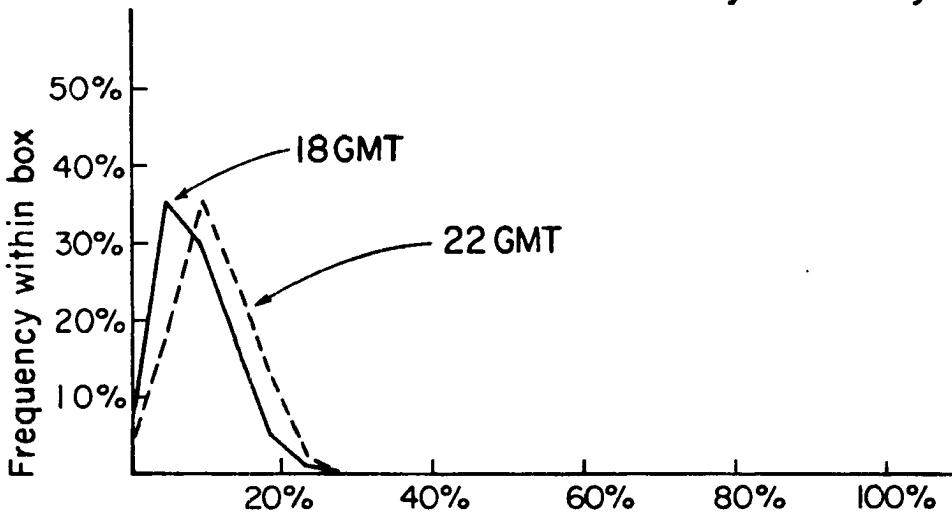


18 GMT Average Frequency = 3.5 %

22 GMT Average Frequency = 5.5 %

Fig. 21. Fraction of month cloudy versus frequency within box from infrared composites for 18 and 22 GMT (11 AM and 3 PM, Local Time) June 1980.

Fraction of month cloudy      July 1980



18 GMT Average Frequency = 8.5 %

22 GMT Average Frequency = 10.5 %

Fig. 22. Fraction of month cloudy versus frequency within box from infrared composites for 18 and 22 GMT (11 AM and 3 PM, Local Time) July 1980.

is instructive, Figs. 15-22 provide a clearer display of the distribution and magnitude of cloud frequency over the region.

In all except the July 1980 comparison of visible composites, the average cloud frequency for 22 GMT was clearly greater than for 18 GMT. Thus, a quantitative analysis of the composite imagery confirms the hypothesis and the qualitative results that the 22 GMT imagery exhibits more overall cloudiness than occurs in the 18 GMT composites.

### III.C.2 Month-to-Month Variations

Some month-to-month variations in the composite imagery were expected because over the period of a month changes in the long wave upper air patterns and jet stream positions can be quite significant. While in northern Colorado one might expect a slightly higher frequency of thunderstorms in July compared to June, the situation in the northern High Plains could be different. In any event, evidence of migration of cloudiness from one region to another due to changes in the long wave pattern ought to appear when June and July composites are compared. After examining the June and July composites, it becomes clear that the differences are probably not the same from year to year. Month-to-month differences in 1979 are not the same as those in 1980. The 1979 18 GMT composites show fairly well defined bright centers about the formerly listed significant mountain regions, with more cloudiness in the Dakotas in July; but the 22 GMT imagery for June and July 1979 seem to be opposites or negatives of one another, with the preferred regions for cloudiness in June appearing suppressed in July 1979, with the exception of a few spots downwind of the significant topographic features. In short, for 1979 the 18 GMT composites are similar, but the

22 GMT composites show a clear migration of the preferred and suppressed regions of cloudiness. In 1980 systematic differences between June and July imagery are well defined. In June 1980, clouds formed with the greatest frequency northwest of a diagonal from south central Wyoming to just west of Regina. In July 1980 clouds were not as restricted to any one area, but cloud formation appears to have been suppressed over the entire region; hence, clouds formed primarily in the few regions where topography favors convergence and provides lifting necessary for convection. These month-to-month differences in the 1980 composite imagery are present at both 18 GMT and 22 GMT. While month-to-month variations in the composites exist, they are not manifest in simple relationships that are the same for the two years examined. In light of the strong large scale synoptic differences between the 1979 and 1980 summer seasons, absence of consistent month-to-month variations of cloud frequency and location in the composite imagery is not unreasonable.

Simple systematic month-to-month variations do not emerge when the composites are quantitatively analyzed, either. Figures 23-38 show the variation of the number of pixels with any cloud frequency for the four quadrants of a 256 by 256 pixel box<sup>10</sup> centered at Miles City, Montana. For the 18 GMT visible imagery, the average cloud frequency over the box is greater in June than in July for both 1979 and 1980; however, this is not true for the 18 GMT infrared composites and both the 22 GMT visible and the 22 GMT infrared composites. Presence in the box of the ridgy area south and southwest of Miles City may confound month-to-month

---

<sup>10</sup>Recall that the COMTAL screen dimensions are 512 by 512.

18 GMT Visible June 1979  
frequency within quadrant

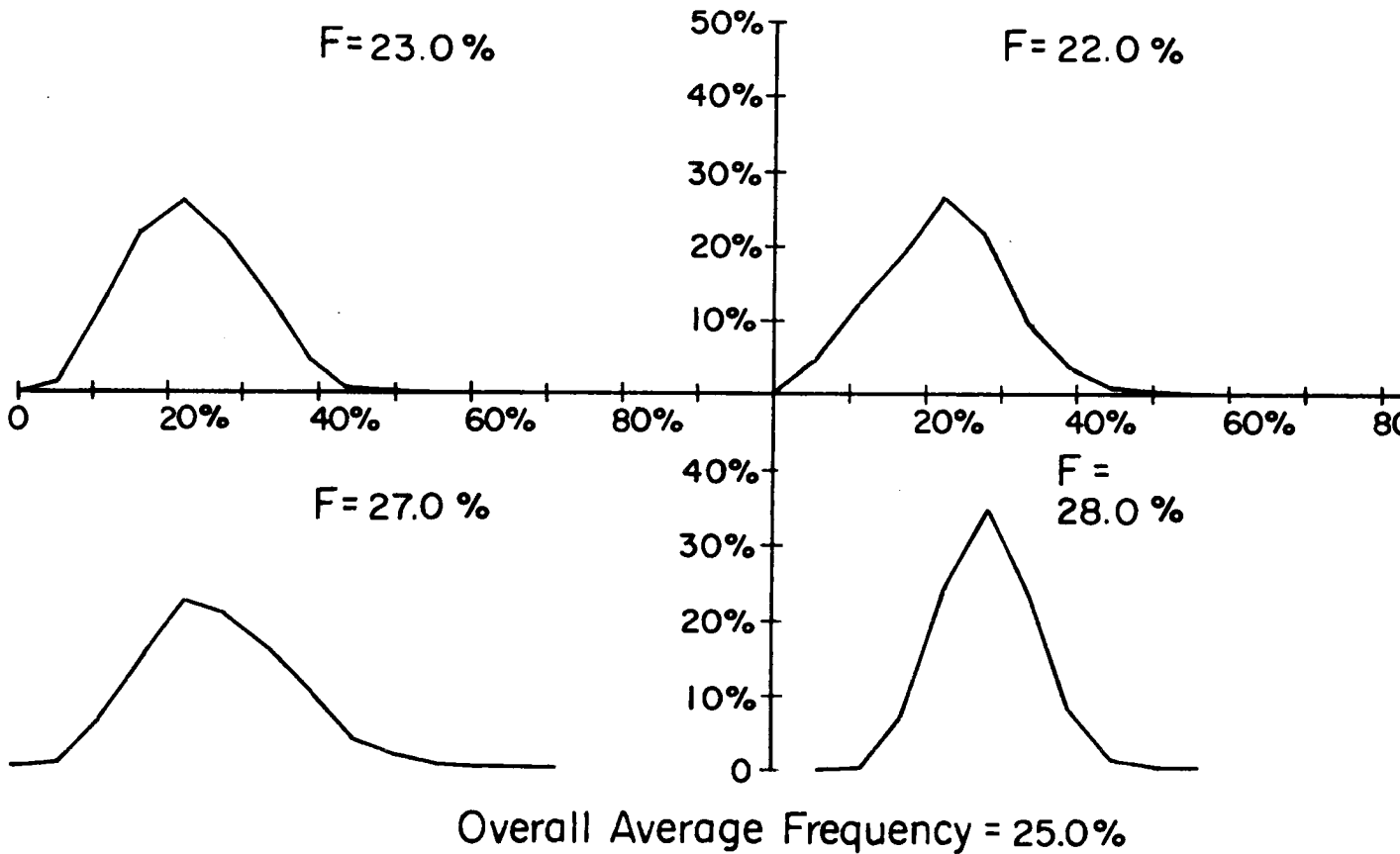


Fig. 23. Fraction of month cloudy versus frequency within quadrant for 18 GMT, visible composite. The average cloud frequency (F) for the northwest, southwest, and southeast quadrants is shown in each respective quadrant.

# 22 GMT Visible June 1979

frequency within quadrant

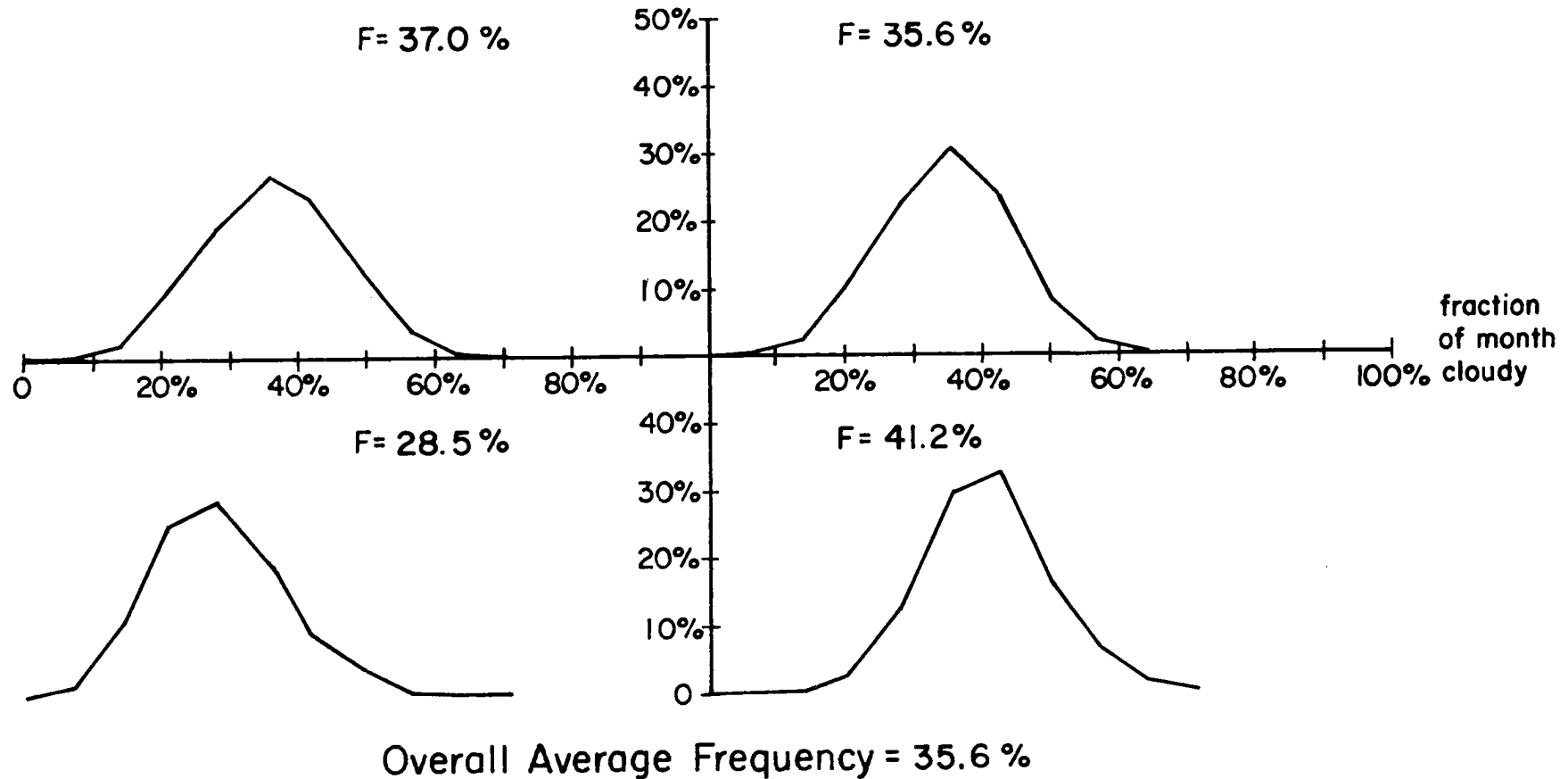


Fig. 24. Fraction of month cloudy versus frequency within quadrant for 22 GMT, June 1979 visible composite. The average cloud frequency (F) is shown for each quadrant.

18 GMT Visible July 1979  
frequency within quadrant

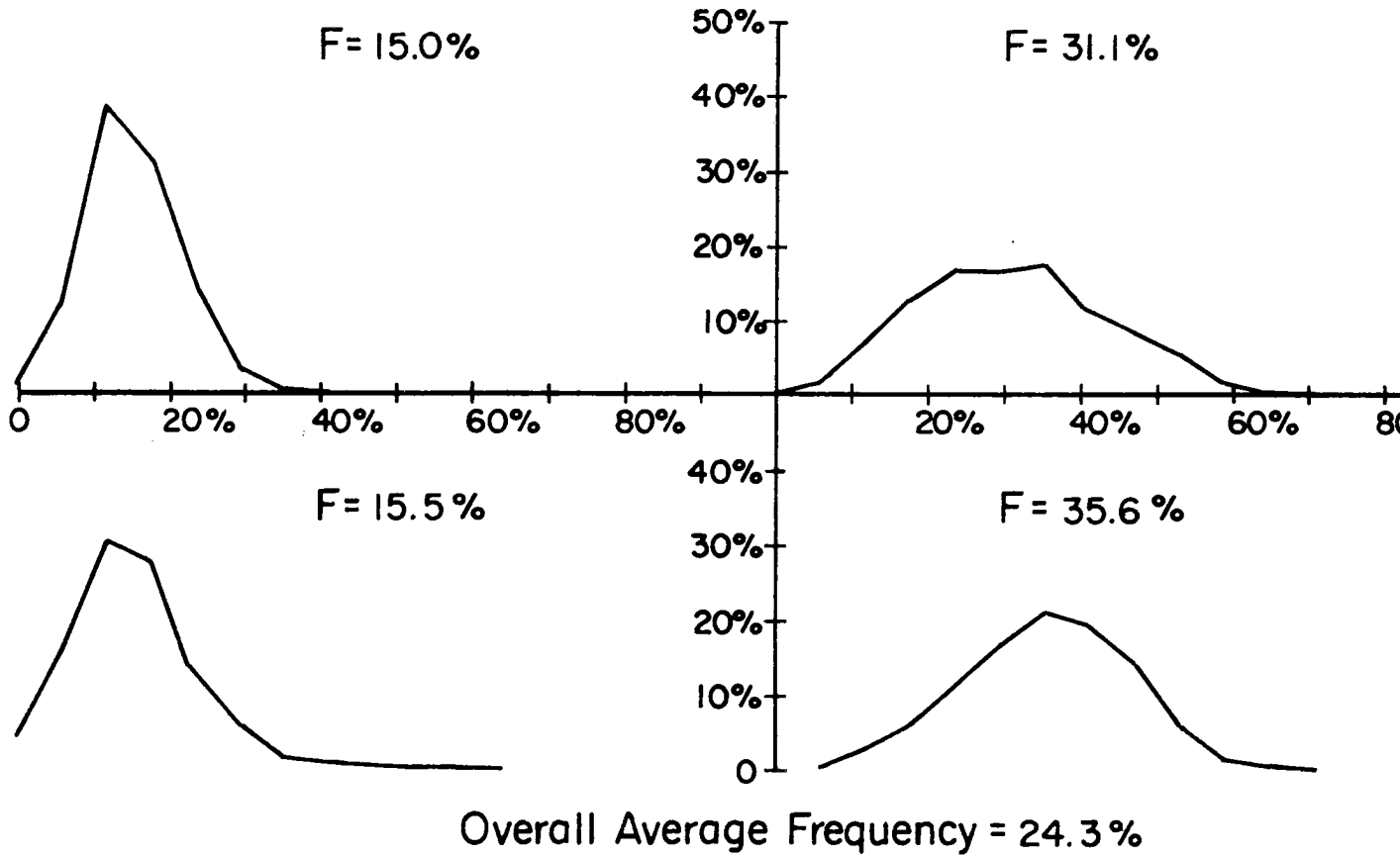


Fig. 25. Fraction of month cloudy versus frequency within quadrant for 18 GMT, visible composite. The average cloud frequency (F) is shown in each q

22 GMT Visible July 1979  
frequency within quadrant

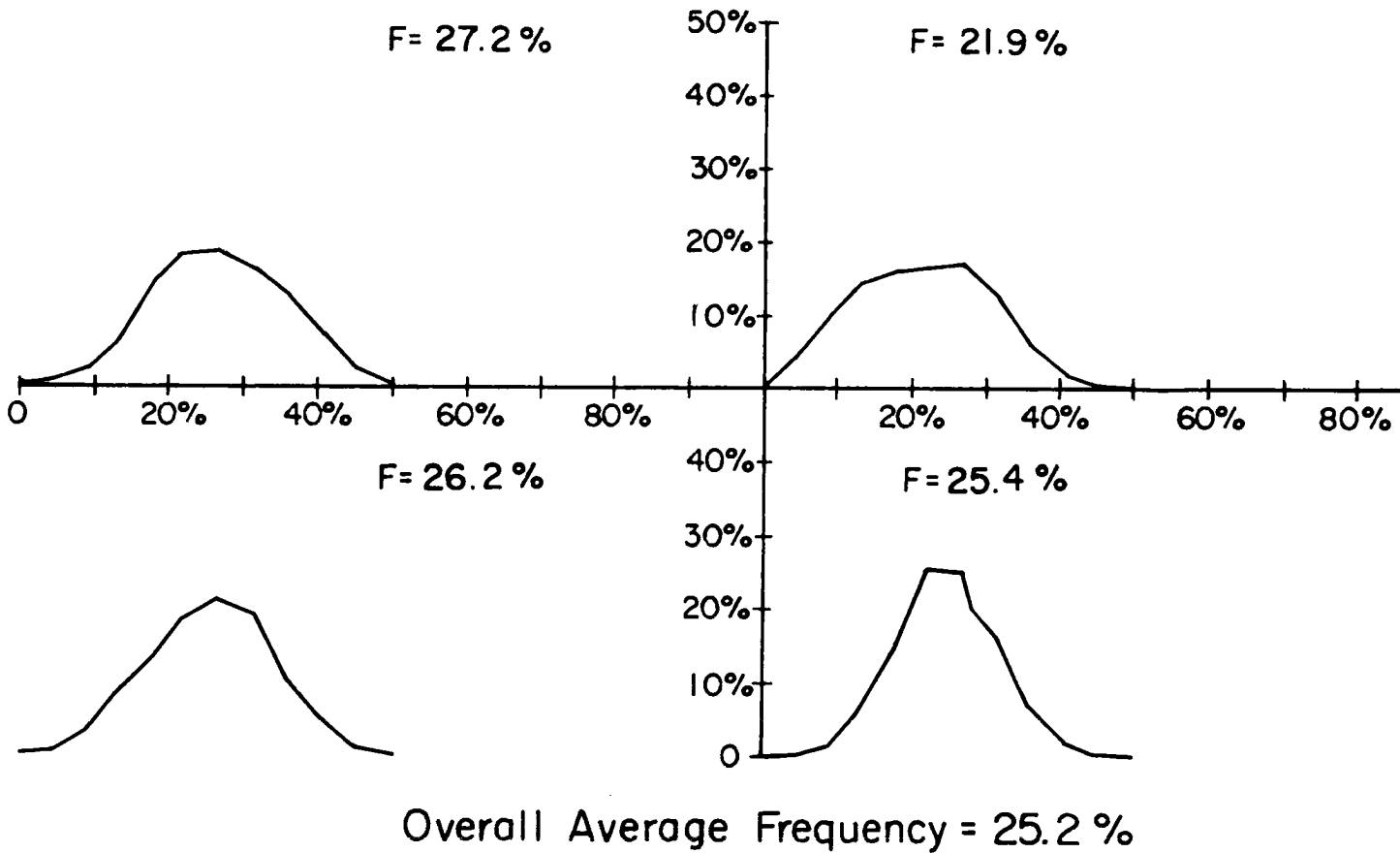


Fig. 26. Fraction of month cloudy versus frequency within quadrant for 22 GMT, July 1979 visible composite. The average cloud frequency (F) is shown for each quadrant.

18 GMT Visible June 1980  
frequency within quadrant

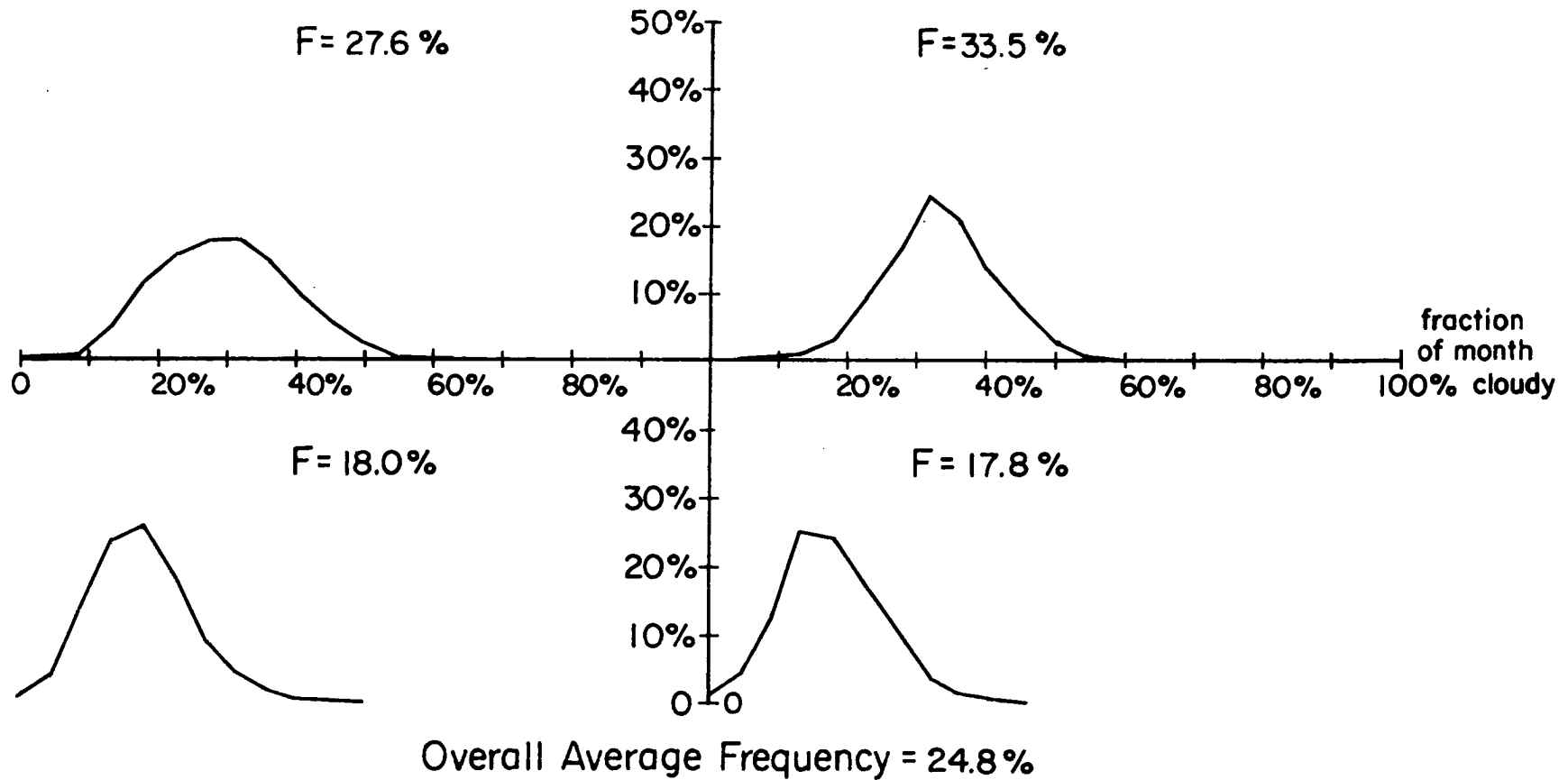


Fig. 27. Fraction of month cloudy versus frequency within quadrant for 18 GMT, June 1980 visible composite. The average cloud frequency (F) is shown in each quadrant.

# 22 GMT Visible June 1980

frequency within quadrant

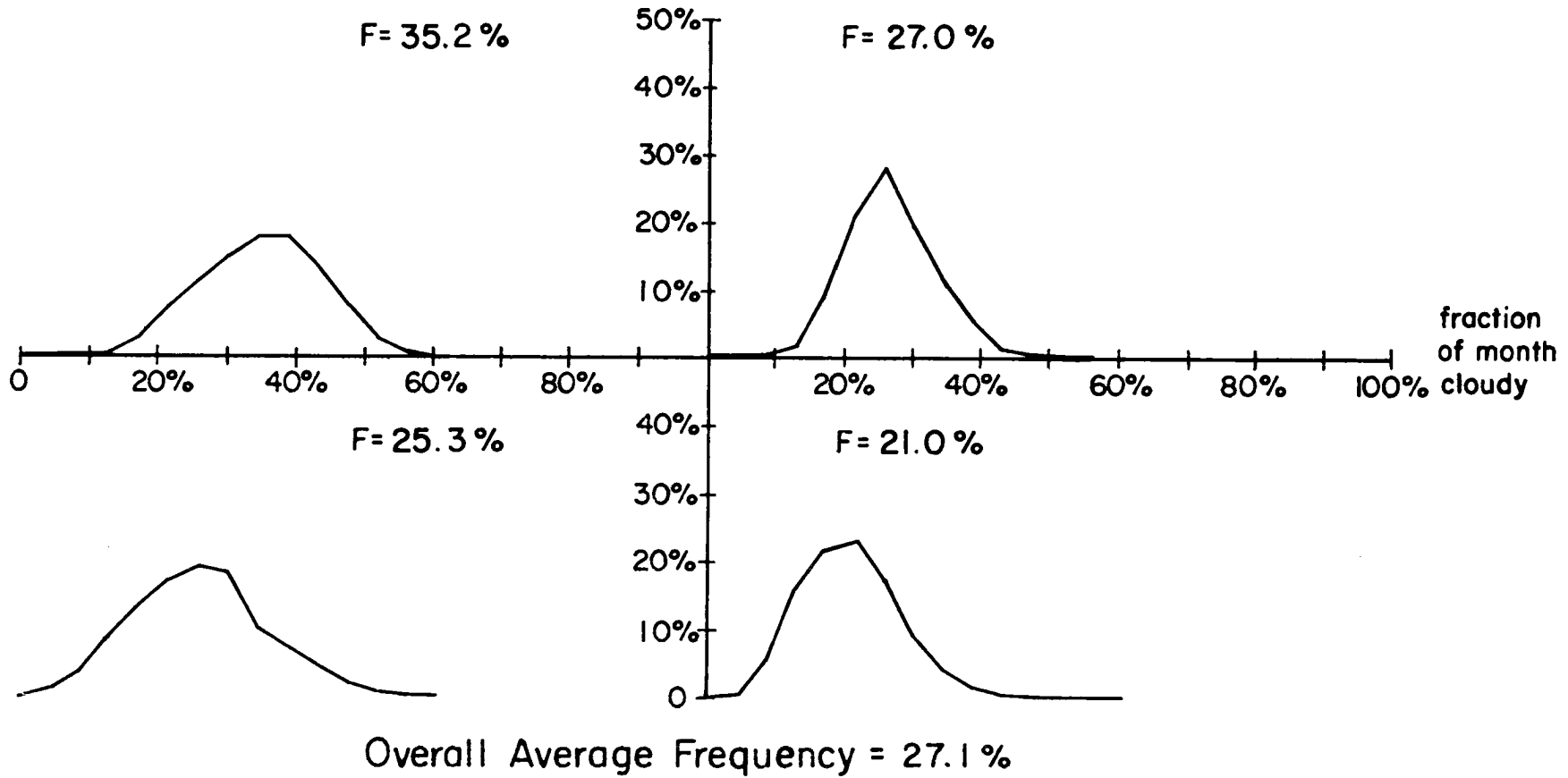


Fig. 28. Fraction of month cloudy versus frequency within quadrant for 22 GMT, June 1980 visible composite. The average cloud frequency (F) is shown for each quadrant.

18 GMT visible July 1980  
frequency within quadrant

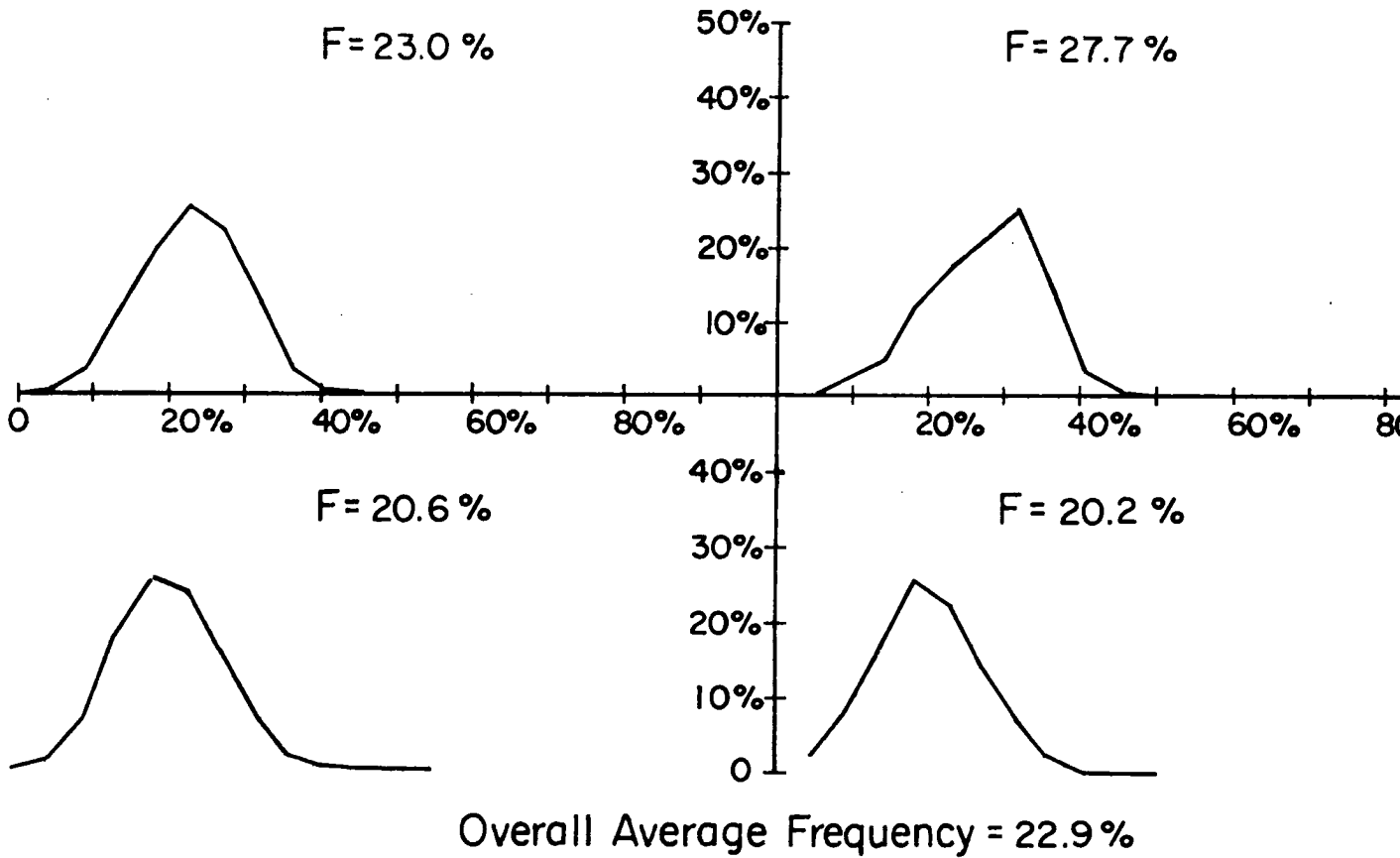


Fig. 29. Fraction of month cloudy versus frequency within quadrant for 18 GMT, visible composite. The average cloud frequency ( $\bar{F}$ ) is shown in each quadrant.

# 22 GMT Visible July 1980

frequency within quadrant

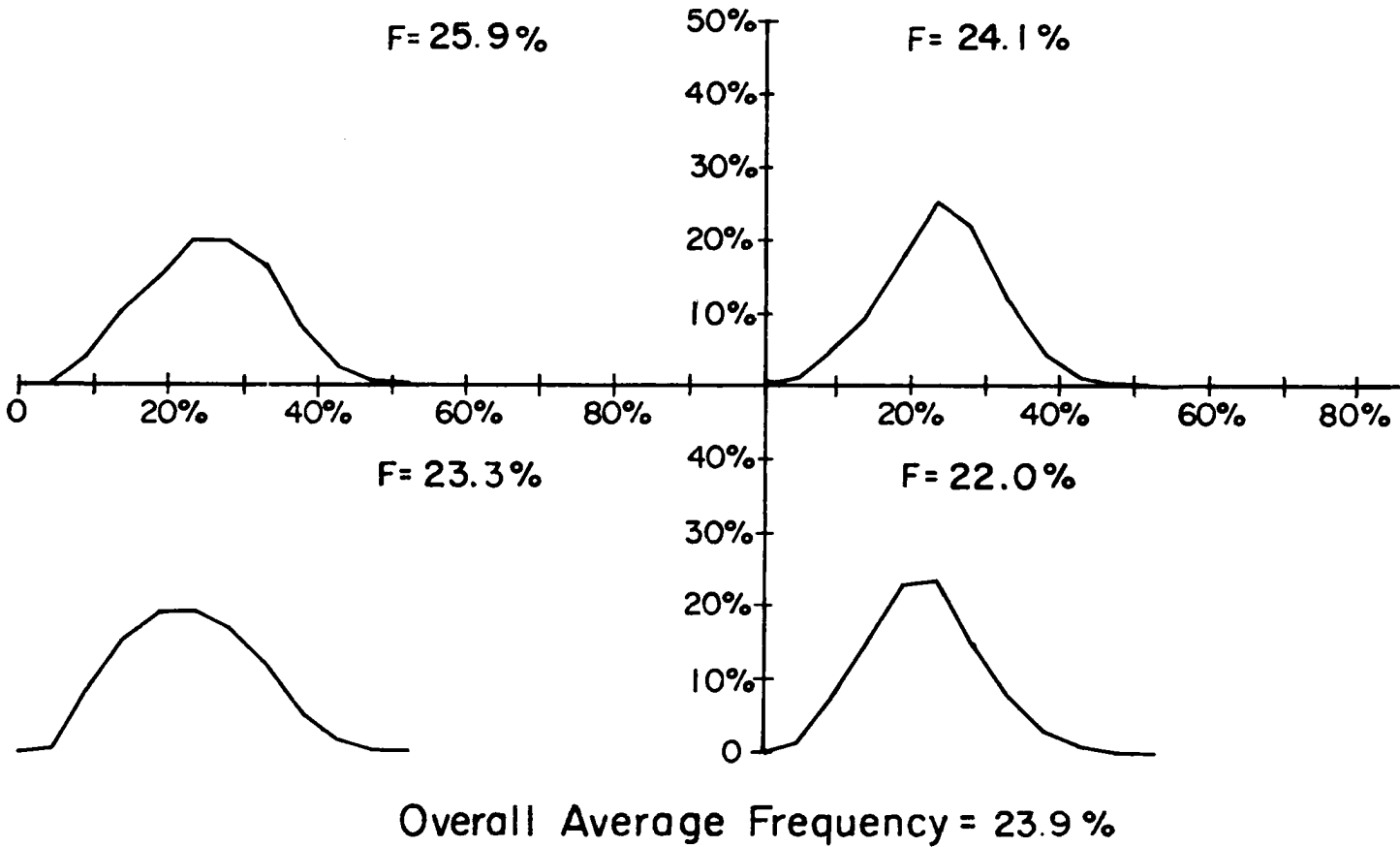
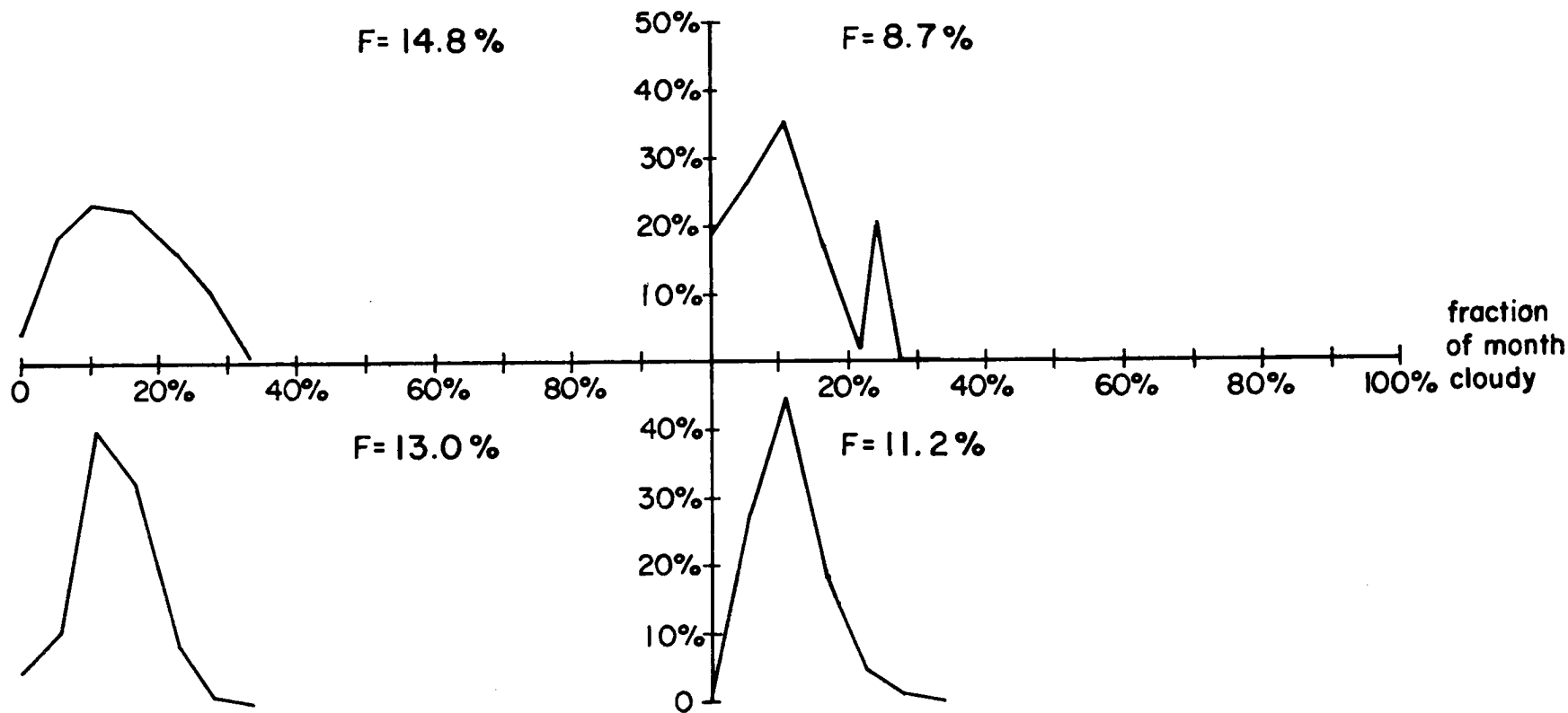


Fig. 30. Fraction of month cloudy versus frequency within quadrant for 22 GMT, July 1980 visible composite. The average cloud frequency (F) is shown for each quadrant.

# 18 GMT Infrared June 1979

frequency within quadrant



**Overall Average Frequency = 11.9 %**

Fig. 31. Fraction of month cloudy versus frequency within quadrant for 18 GMT, June 1979 infrared composite. The average cloud frequency (F) is shown for each quadrant.

# 22 GMT Infrared June 1979

frequency within quadrant

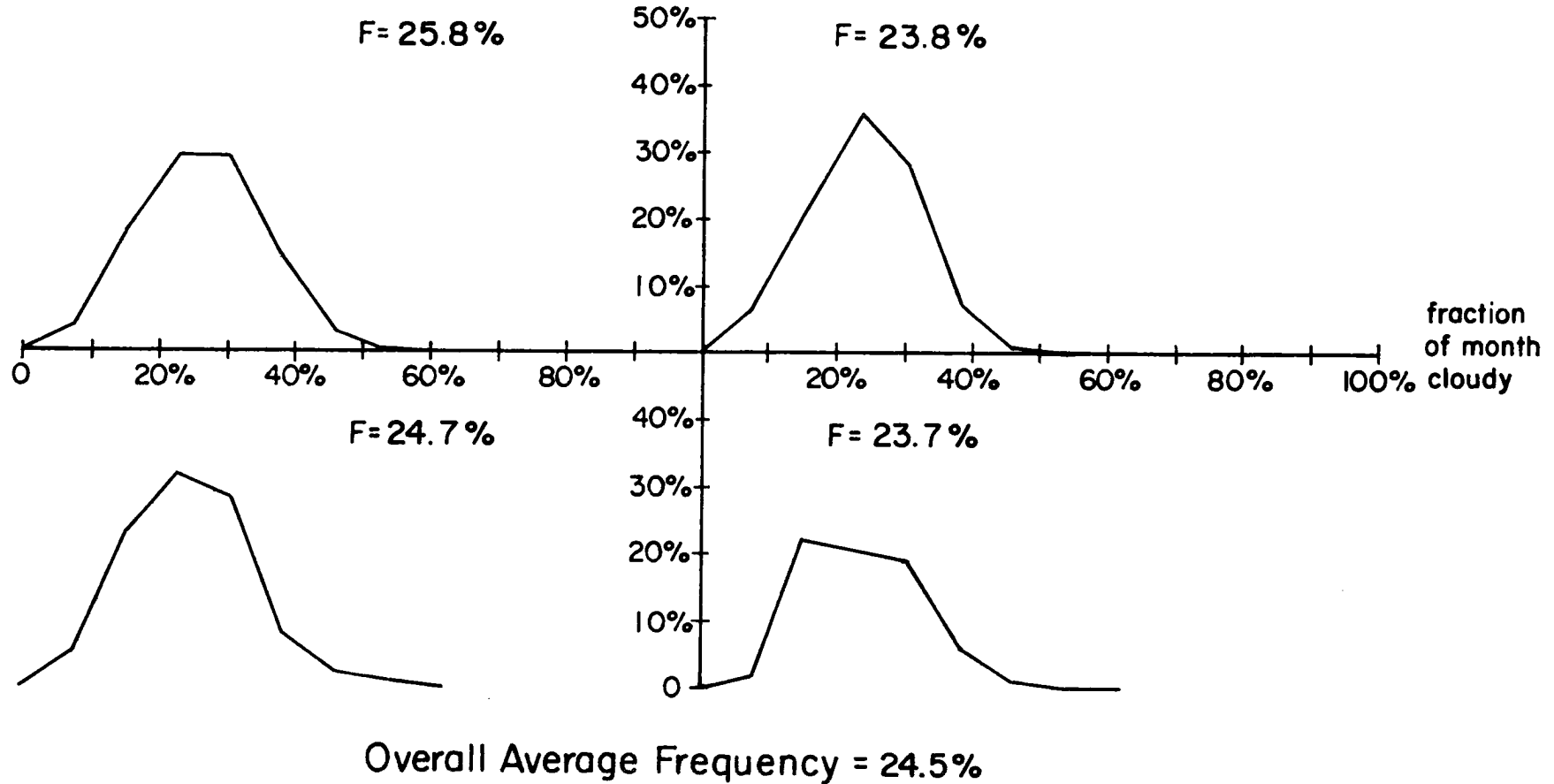


Fig. 32. Fraction of month cloudy versus frequency within quadrant for 22 GMT, June 1979 infrared composite. The average cloud frequency (F) is shown for each quadrant.

18 GMT infrared July 1979  
frequency within quadrant

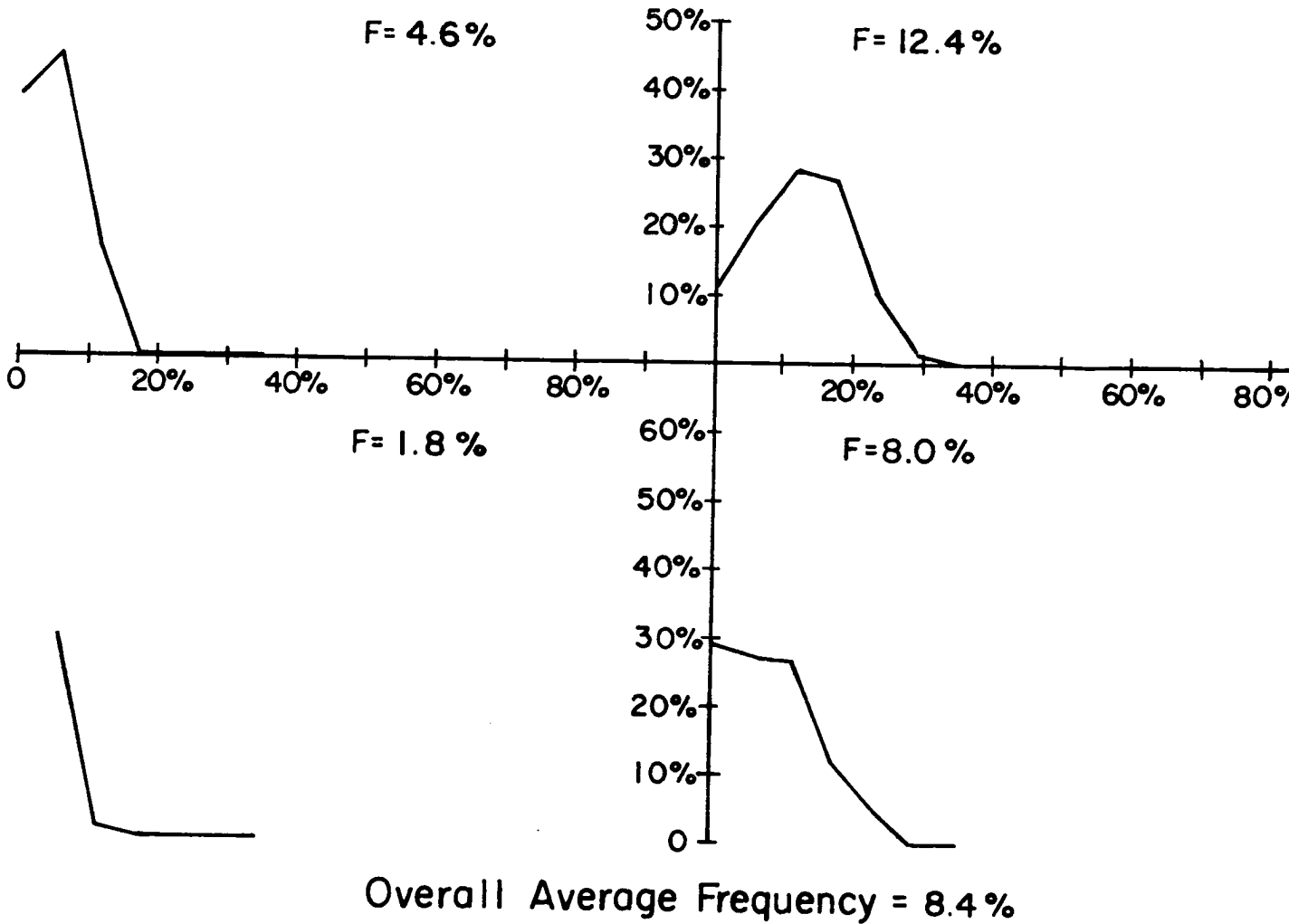


Fig. 33. Fraction of month cloudy versus frequency within quadrant for 18 GMT, July 1979 infrared composite. The average cloud frequency (F) is shown for each

# 22 GMT Infrared July 1979

frequency within quadrant

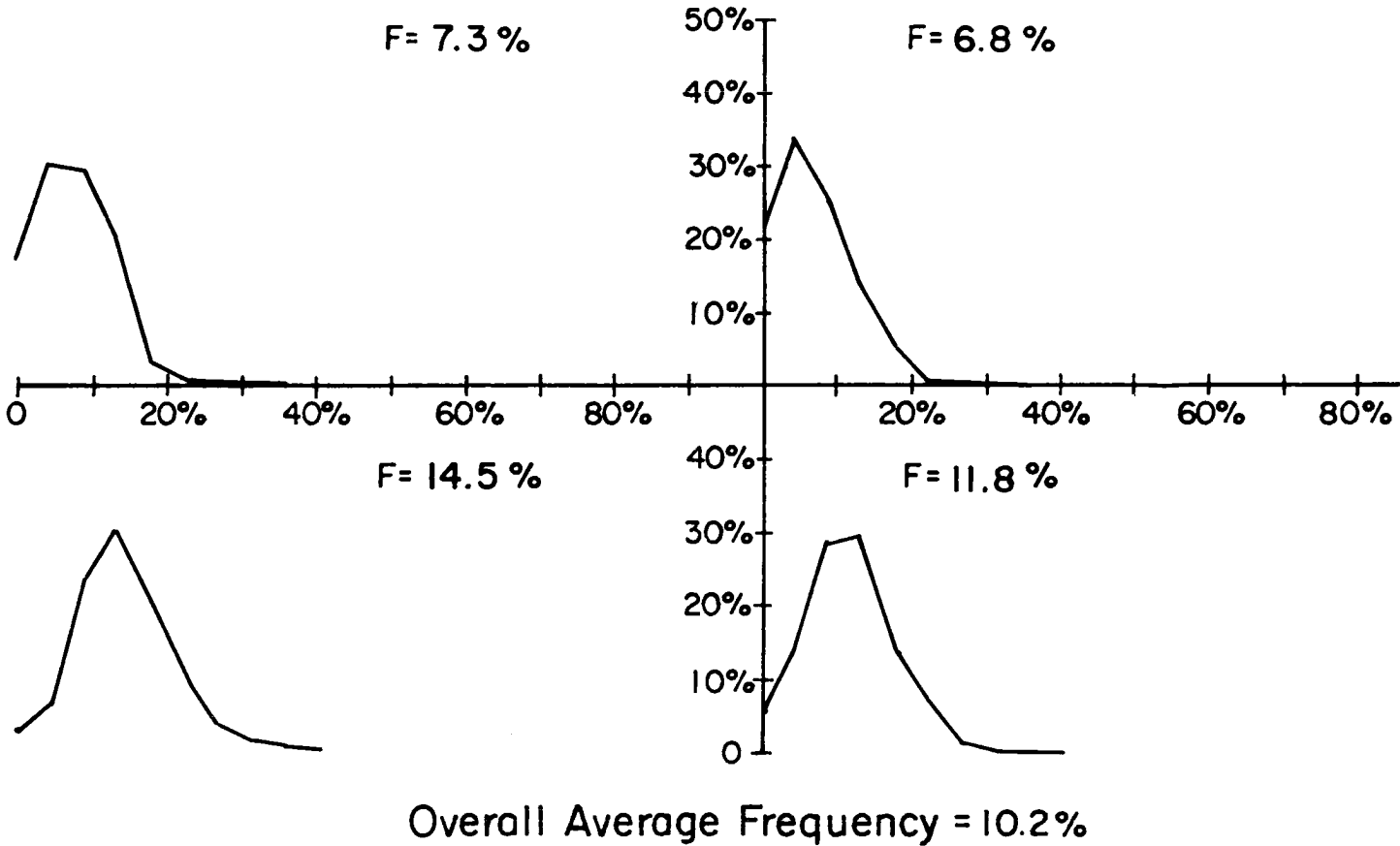


Fig. 34. Fraction of month cloudy versus frequency within quadrant for 22 GMT, July 1979 infrared composite. The average cloud frequency (F) is shown for each quadrant.

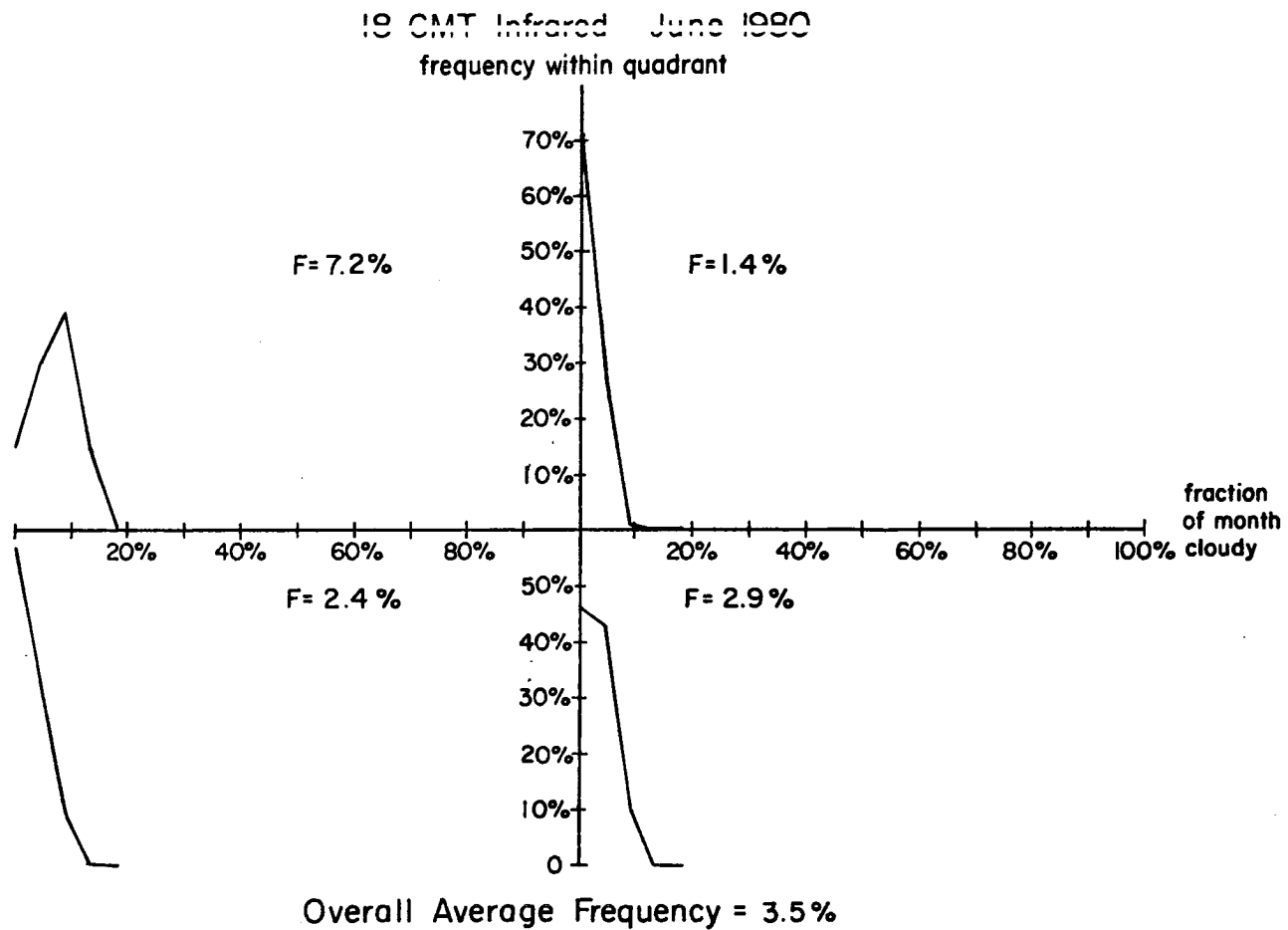


Fig. 35. Fraction of month cloudy versus frequency within quadrant for 18 GMT June 1980 infrared composite.

22 GMT Infrared June 1980

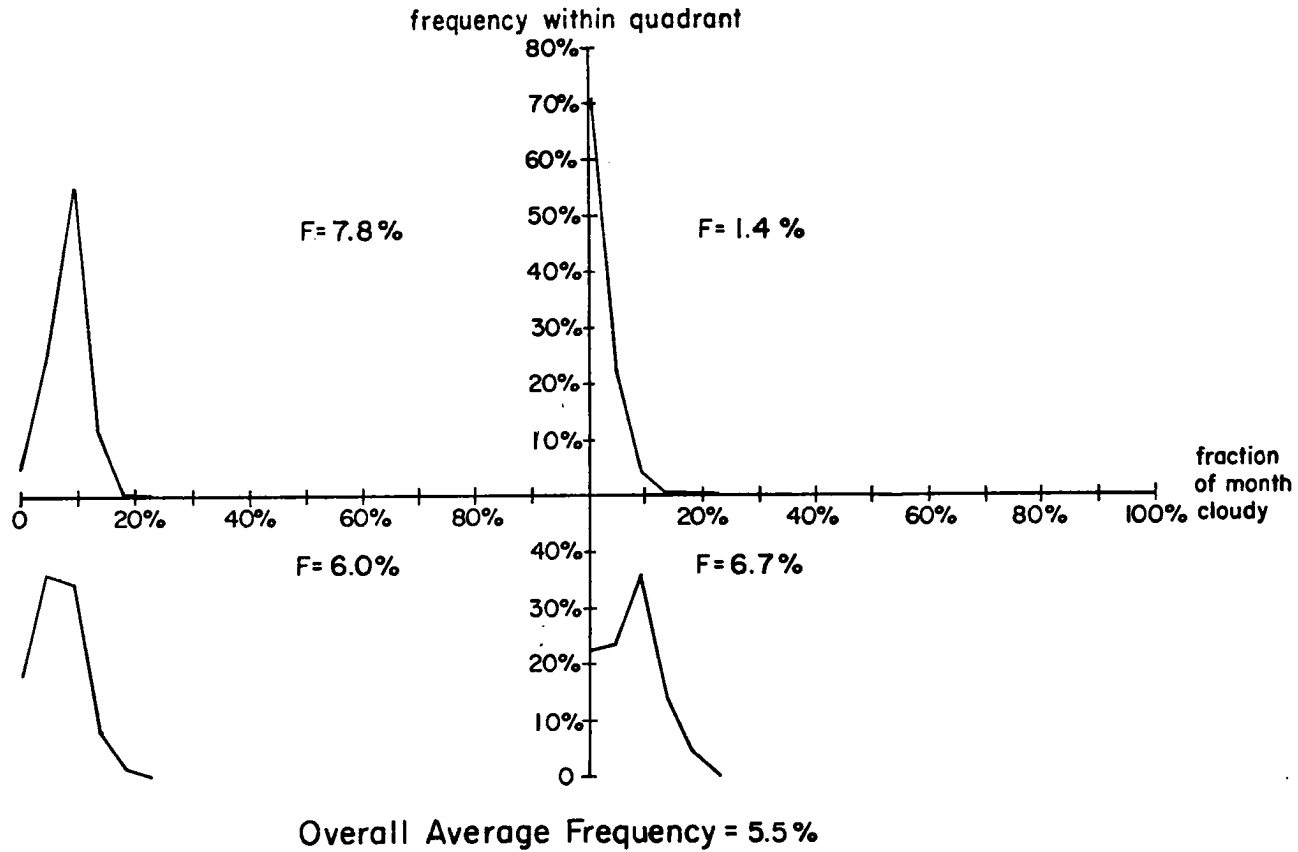
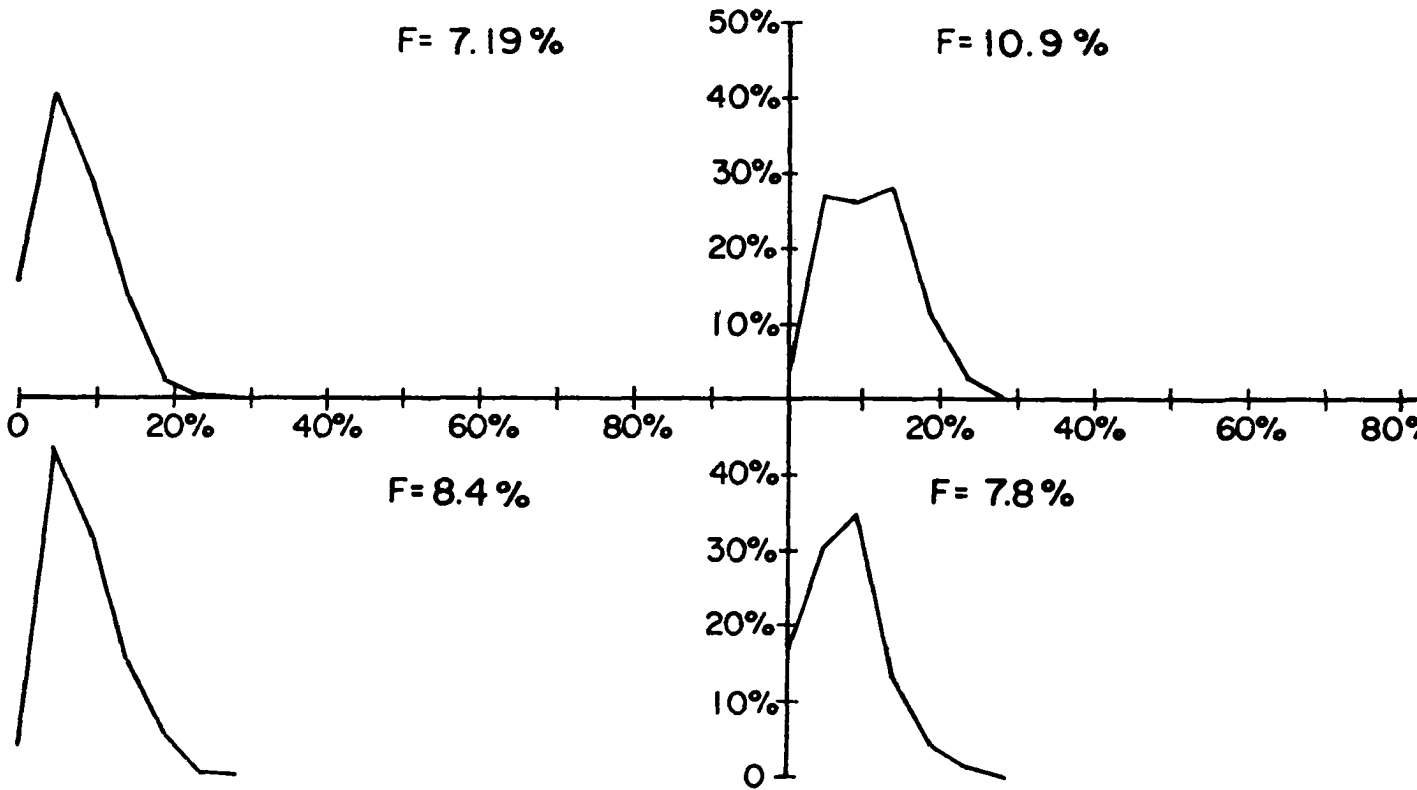


Fig. 36. Fraction of month cloudy versus frequency within quadrant for 22 GMT June 1980 infrared composite.

# 18 GMT Infrared July 1980

frequency within quadrant



**Overall Average Frequency = 8.5%**

Fig. 37. Fraction of month cloudy versus frequency within quadrant for 18 GMT, July infrared composite. The average cloud frequency (F) is shown for each quadrant.

22 GMT Infrared July 1980  
frequency within quadrant

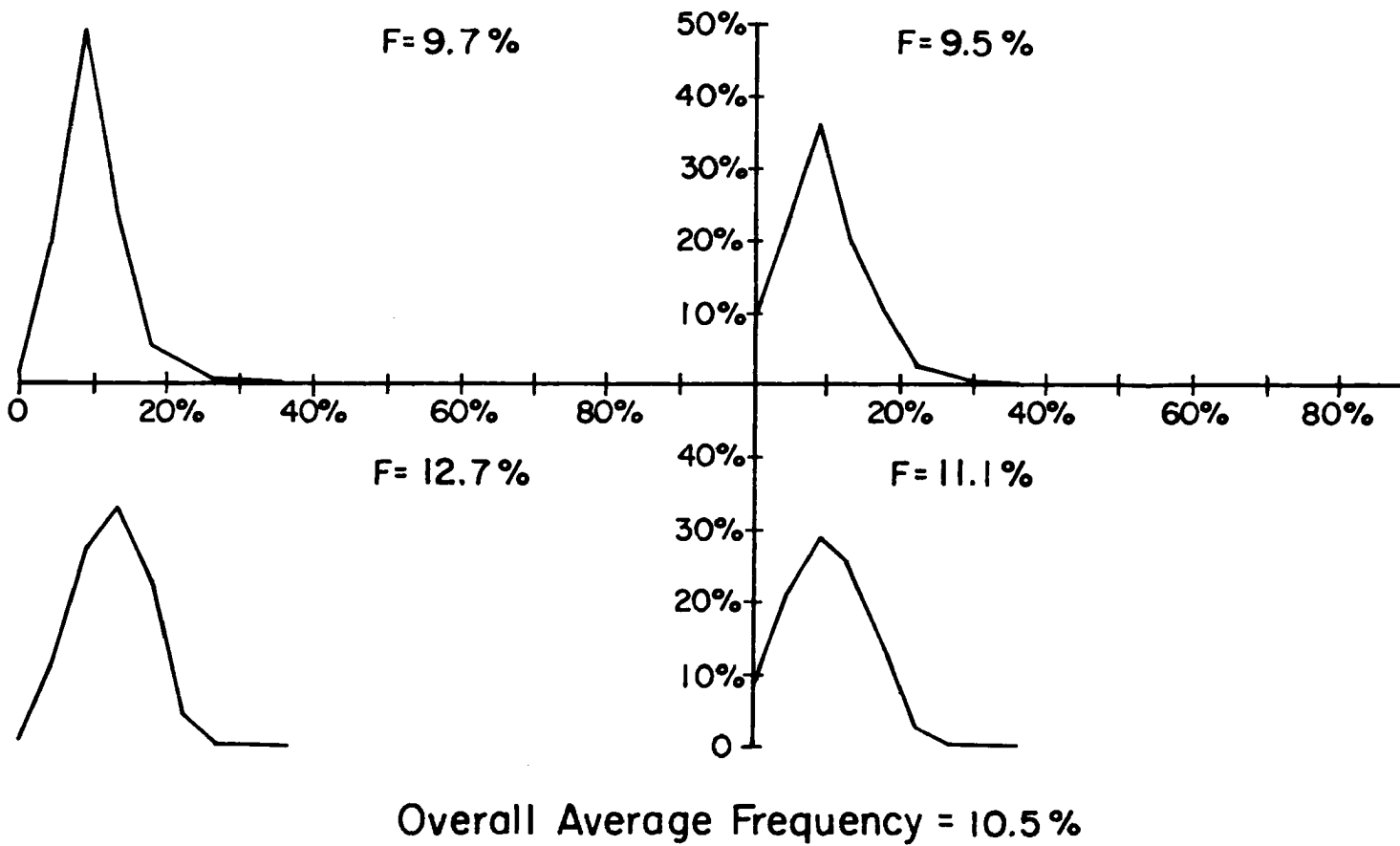


Fig. 38. Fraction of month cloudy versus frequency within quadrant for 22 GMT, July 1980 infrared composite. The average cloud frequency (F) is shown for each quadrant.

comparisons of overall cloud frequency. Since the hypothesis for month-to-month variations includes migration of preferred regions of cloudiness, Figs. 23-38 should be examined in this light. For example, the quadrant with the highest average cloud frequency is the upper left for all the 18 GMT visible composite imagery, but for the 18 GMT infrared composites, the quadrant with the highest average cloud frequency moves from the upper left in June to the upper right in July, in both years. The 22 GMT infrared composites have their highest average cloud frequency in the upper left quadrant in June and in the lower left quadrant in July. All these observations support a hypothesis for systematic month-to-month migration of the preferred regions of cloudiness, although other observations of the quantitative analysis do not. The quadrants with the highest cloud frequency for the 22 GMT visible composites, for example, go from lower right in June to upper left in July for 1979, whereas the highest average cloud frequency stays in the upper left quadrant for June and July 1980. Such month-to-month variations in cloud frequency and location in the quantitative analysis of the composites tend to support the hypothesis, but do not conclusively identify systematic month-to-month migrations of cloudiness. If month-to-month variations in cloud frequency and location normally do exist, the stagnant high pressure in the region during 1980 may have prevented normal monthly patterns from emerging. Two years of satellite data, while better than a few days, probably does not constitute a sufficient climatology to generalize about typical month-to-month cloudiness migration patterns, especially when one year is very atypical. Yet, it is clear that the cloud frequencies and locations in the composite imagery do change from month-to-month.

### III.C.3 Year-to-Year Variations

The summer of 1980 broke many high temperature records over much of the central United States. As mentioned before, stagnant high pressure persisted over the Great Plains, serving to suppress vertical motion and dry the atmosphere. Because of the drought, the 1980 composites should have generally lower cloud frequencies. However, the mountains along the lee slopes of the Rockies, being the major source of uplift, could dominate in inducing convection in 1980, whereas in a wetter year, like 1979, the general overall availability of moisture might be conducive to more widespread cumulus development.

A cursory look at the composite imagery (Figs. 7a-14b) seems to verify the hypothesis that the 1980 composites ought to show less cloudiness than in 1979. In June 1980, most cloudiness seemed to be concentrated in the upper left portion of the area (northwestern Wyoming, western Montana, and the western part of Canada) with convection in the Dakotas, eastern Montana, eastern Wyoming, and especially Nebraska, greatly suppressed. The July 1980 composites are generally darker than June's and convection seems to be suppressed even in the northern and western parts of the area by July. When the 1980 composites are compared with respective 1979 imagery, the 1979 imagery exhibits more cloudiness in every case. Due to the suppressive conditions that caused the 1980 midwestern drought, this conclusion is not astonishing.

Since qualitatively examining the composites seems to verify the hypothesis that 1980 should reflect the drought, the quantitative results from examining the 256 by 256 pixel box centered at Miles City are quite curious. In only three of the eight comparisons (18 GMT June infrared, 22 GMT July visible, and 22 GMT June infrared) is the average cloud

frequency over the box greater in 1979 than in 1980. The implications of the quantitative analysis are valid only for the local area around Miles City, which includes a secondary topographic region of enhanced convective development. While the effects of the 1980 drought were felt in Miles City, clouds still developed there, perhaps aided by moisture from the Yellowstone River, Tongue River, or local agricultural irrigation. Clouds are necessary for precipitation, but of course they are not sufficient. Although convection was suppressed during summer 1980, the frequency of cloudiness in the Miles City area was not severely affected. This could be good news for those interested in developing a precipitation enhancement weather modification program for the Miles City region.

#### IV. INTERPRETING TEMPORAL VARIATIONS WITH AVAILABLE WEATHER DATA

The stagnant high pressure that caused the drought of 1980 has been mentioned previously. The 12 GMT surface and 500 mb maps published by the United States Department of Commerce were examined to note differences in surface moisture and upper-air trough passages between the two months and the two years. These synoptic observations serve to better explain the temporal variations observed in the composites. They also resolve why, in some cases, the temporal variations differed from those expected in the hypotheses.

First consider the 500 mb pattern. In June 1979 at least three major troughs, and several short waves, travelled through the atmosphere above Miles City. July 1979 saw a total of at least four troughs, and again, several short waves<sup>11</sup> that passed over the area. In June 1980, two troughs and a few short waves crossed Miles City; but in July 1980, only one upper air trough passed over the region, and that was late in the month. In total, at least seven 500 mb troughs and numerous short waves crossed the northern High Plains in 1979; whereas in 1980 only three 500 mb troughs travelled through. High pressure dominated the High Plains in 1980; fewer troughs passed; and higher temperatures and minimal precipitation were the rule for the area in 1980, especially during July.

---

<sup>11</sup>Detection of short waves is difficult when only one map per day is consulted. The marked upper air differences between the two years is clear even if short waves are ignored.

Surface moisture at 12 GMT at Miles City, Montana, Lewistown, Montana, Billings, Montana, and Rapid City, South Dakota, was examined to see if the variation in moisture availability might explain some of the temporal variations in the composites. The average 12 GMT surface temperature, dewpoint, and dewpoint depression in degrees Fahrenheit for these four reporting stations over the four months is shown in Table 3. At each of these four stations the surface moisture for June 1979 was less than that for 1980. This helps explain why, in quantitatively analyzing the year-to-year variations in cloud frequency, the June 1980 visible composites did not have lower average cloud frequencies than in June 1979, as was expected. The average surface moisture in July 1979 was much higher at all four stations than in July 1980, and this is consistent with the qualitative and quantitative comparisons of cloud frequency. The hypothesis that all the 1980 composites ought to be darker than the respective 1979 composites was a bit simplistic in that it assumed the drought began earlier, meaning less moisture was available in June 1980 than in June 1979. Table 4 demonstrates that this assumption is not true; more moisture was available for convection over the region in June 1980 than in June 1979.

Moisture alone does not explain the variations in average cloud frequency. The four months may be ranked from wettest to driest, based on average dewpoint, average dewpoint depression, or a combination of these two, such as average dewpoint minus average dewpoint depression (see Table 5). Yet, when the months are ranked by their average cloud frequency over the 256 by 256 pixel box centered at Miles City, in no case do they correlate exactly with any of the moisture rankings.

Table 6

Ranking the Months by Average Cloud  
Frequency in the Composite Imagery

5a. Ranking by Averaging All Cloud  
Frequencies (18 and 22 GMT, Visible and Infrared)

1. June 1979 (23.5%)
2. July 1979 (17.1%)
3. July 1980 (16.5%)
4. June 1980 (15.9%)

5b. Ranking by Averaging All Visible  
Cloud Frequencies (18 and 22 GMT)

1. June 1979 (29.6%)
2. June 1980 (26.0%)
3. July 1979 (24.8%)
4. July 1980 (23.4%)

5c. Ranking by Averaging All Infrared  
Cloud Frequencies (18 and 22 GMT)

1. June 1979 (17.2%)
2. July 1980 ( 9.6%)
3. June 1980 ( 9.5%)
4. July 1979 ( 9.4%)

5d. Ranking by 18 GMT Visible Cloud Frequencies

1. June 1980 (32.1%)
2. June 1979 (25.0%)
3. July 1979 (24.3%)
4. July 1980 (22.9%)

5e. Ranking by 18 GMT Infrared Cloud Frequencies

1. June 1979 (11.9%)
2. July 1980 ( 8.5%)
3. July 1979 ( 8.4%)
4. June 1980 ( 3.5%)

5f. Ranking by 22 GMT Visible Cloud Frequencies

1. June 1979 (35.6%)
2. June 1980 (27.1%)
3. July 1979 (25.2%)
4. July 1980 (23.4%)

5g. Ranking by 22 GMT Infrared Cloud Frequencies

1. June 1979 (24.5%)
  2. July 1979 (10.2%)
  3. July 1980 (10.5%)
  4. June 1980 ( 5.5%)
-

Perhaps the most natural weather data to compare with the composite imagery is rainfall data, for cloudiness variations roughly parallel rainfall variation (Trewartha, 1968). Because clouds are necessary for rainfall, the potential of using cloud data from satellites to estimate rainfall has been explored. Rainfall estimation schemes have been developed for mid latitudes that utilize satellite data only (Griffith, et al., 1978; Griffith, et al., 1981; Scofield and Oliver, 1977; Scofield and Oliver, 1980; Oliver and Scofield, 1976). Maps of isohyets for Montana, Wyoming, North Dakota, and South Dakota were compared with the composite imagery. Although a quantitative analysis was not undertaken, rainfall peaks usually coincided with centers of high cloud frequencies, especially at 22 GMT. A detailed comparison of cloud frequency and rainfall deserves further attention. However, because it would not help identify topographic features that initiate convective development, a quantitative comparison of cloud frequency and rainfall data was not performed. Future compositing studies may explore more deeply the relationship between observed cloud frequencies and precipitation.

## V. PREVIOUS CLOUD CLIMATOLOGICAL STUDIES

While the technique of compositing digital satellite data is new, analyzing satellite data to learn about the frequency, location, and distribution of clouds on the High Plains is not. The technique and results from this study will be compared with earlier satellite imagery analysis methods and their results.

To date, three reports on cloud climatological studies of satellite data over the High Plains have been published. The first study (Reynolds and Vonder Haar, 1975) included data collected from May-August 1972-1974. If convective clouds were not observed at the three HIPLEX target sites (Miles City, Montana; Colby, Kansas; and Big Spring, Texas), the imagery was dropped from the analysis. The climatological study was limited to a  $2^\circ$  by  $2^\circ$  box, centered at each target site. The location, number, size distribution, rate of growth, and direction of movement for clouds in these boxes were studied by breaking the  $2^\circ \times 2^\circ$  box into an array of 49 smaller boxes.

Reynolds and Vonder Haar's analysis methods differ somewhat from the compositing techniques used in this study; only some of their results can be compared to the results from compositing. With some limitations, the cloud count and location results can be compared to the cloud frequency results from this study. Figure 39a shows the cloud count for the 49 boxes within the Miles City target site as percentages of the box with the highest count; Fig. 39b shows these relative cloud

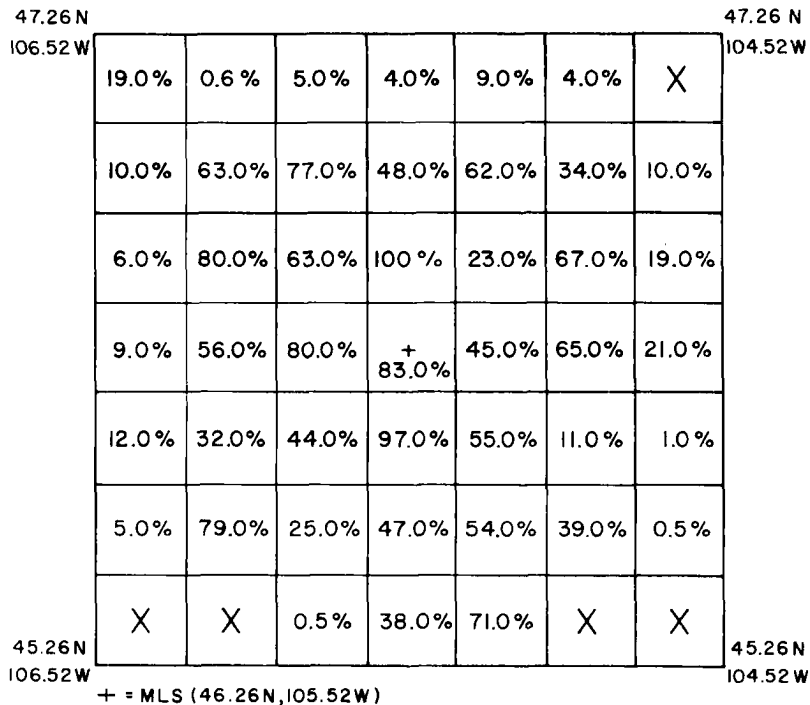


Fig. 39i. Cloud count within the Miles City target site shown as percentages of the box with the highest count, box 3, 4 (from Reynolds and Vonder Haar, 1975).

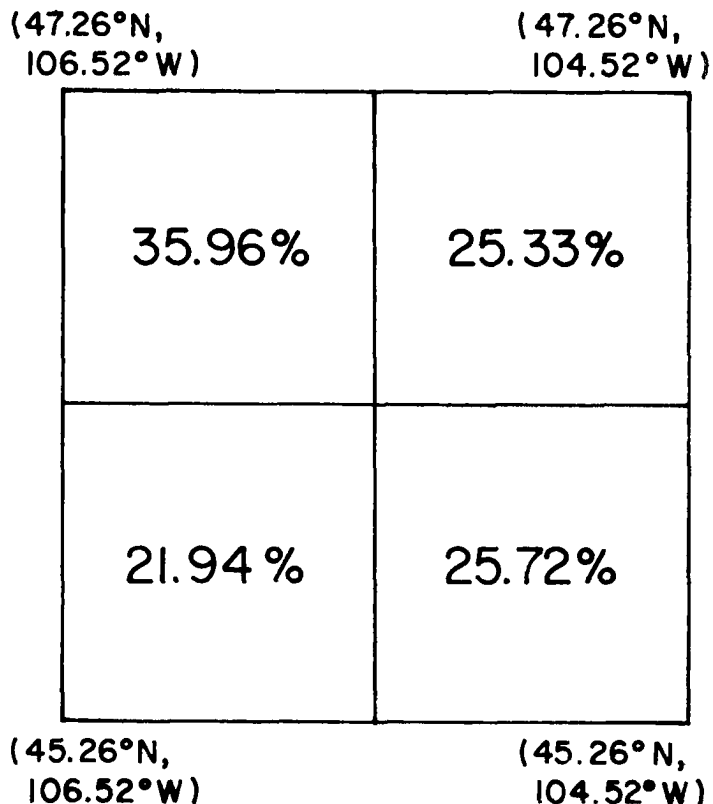


Fig. 39t. Relative cloud count within the Miles City target site averaged by quadrants.

counts averaged by quadrants.<sup>12</sup> Figure 40a shows the distribution of average cloud frequency over the four quadrants of the 256 by 256 pixel box centered at Miles City for the average of the four 18 GMT visible composites. Similarly, Fig. 40b shows the distribution of average cloud frequency (for clouds colder than  $-20^{\circ}\text{C}$ ) over the four quadrants for the average of the four 18 GMT infrared composites. First note that Reynolds and Vonder Haar's analysis counted numbers of clouds, whereas PIXCNT counts the number of pixels with a certain cloud frequency, which subsequently is averaged to get the average cloud frequency for the quadrant as shown in Figs. 40a and 40b. Generally the more clouds in an area, the higher the average cloud frequency ought to be. However, compositing does not count clouds per se. Rather, it determines the frequency of clouds brighter than a certain threshold (chosen to include all convective clouds sensed by the satellite) at every pixel for June and July imagery at 18 and 22 GMT only. Reynolds and Vonder Haar eliminated imagery without convection from their analysis; this experiment used all available imagery (at 18 and 22 GMT) to compute cloud frequencies. Reynolds and Vonder Haar included May and August imagery as well as 15 GMT and 22 GMT imagery in their cloud climatology, but Figs. 40a and 40b are derived using imagery from 18 GMT only. Also, the  $2^{\circ}$  by  $2^{\circ}$  box used by Reynolds and Vonder Haar is smaller than the approximately  $6^{\circ}$  x  $6^{\circ}$  box analyzed in the composites, so some differences can be expected. In both studies, however, the lowest cloud frequencies are observed in the lower left quadrant.

---

<sup>12</sup>These figures were determined by adding the values in the 9 whole boxes in each quadrant and dividing by 9.

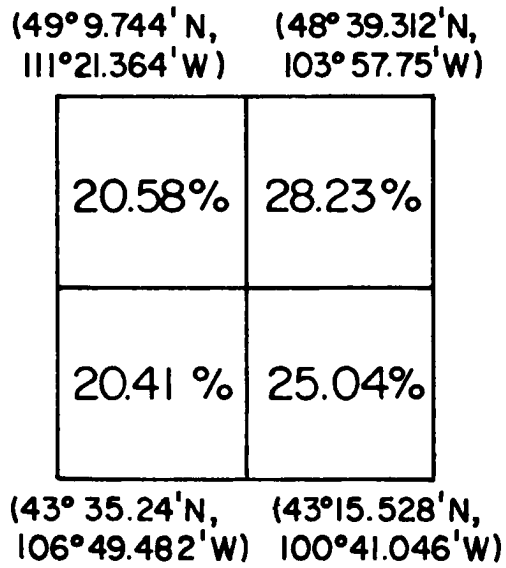


Fig. 40a. Average cloud frequency by quadrant for the average of the 18 GMT visible composites.

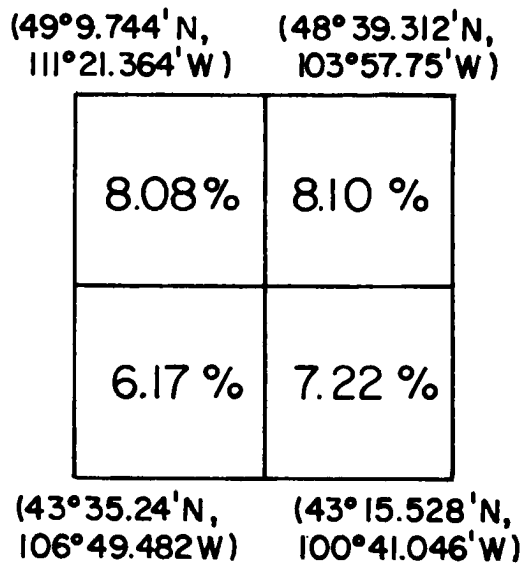


Fig. 40b. Average cloud frequency by quadrant for the average of the 18 GMT infrared composites.

Reynolds and Vonder Haar's second HIPLEX cloud climatology (Reynolds and Vonder Haar, 1978) examined thirty-five days of digital data collected from GOES-West from 24 May - 15 July, 1976. Concentrating on the Miles City area only, this study examined the number, size, location, and temporal frequency of clouds in the region shown in Fig. 41. Of these, only temporal frequency of clouds can be directly compared with the present study, although inferences comparing cloud location in the two studies can also be made. Their plots of time versus number of clouds (Figs. 42 and 43) suggest a 30% increase in cloud number from 18 GMT to 22 GMT for all areas and a 114% increase in cloud number when areas within 175 km of Miles City are considered. Average cloud frequencies

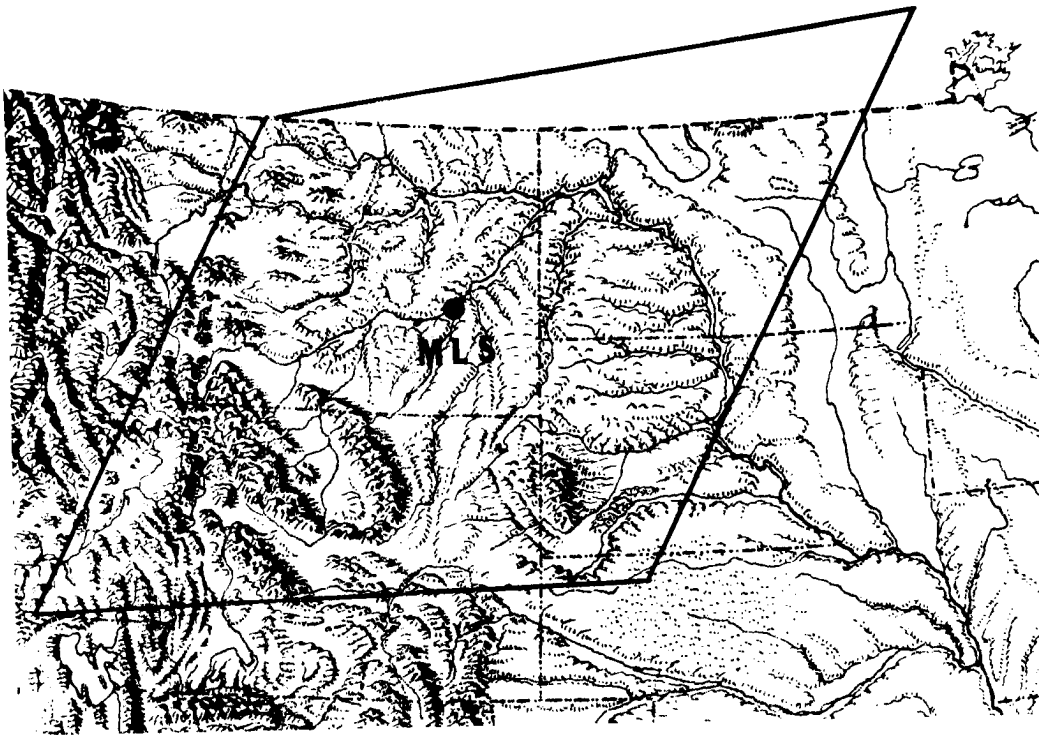


Fig. 41. Area for which the 1976 HIPLEX cloud climatology results are summarized (from Reynolds and Vonder Haar, 1978).

## TIME VS NUMBER OF CLOUDS - ALL AREAS

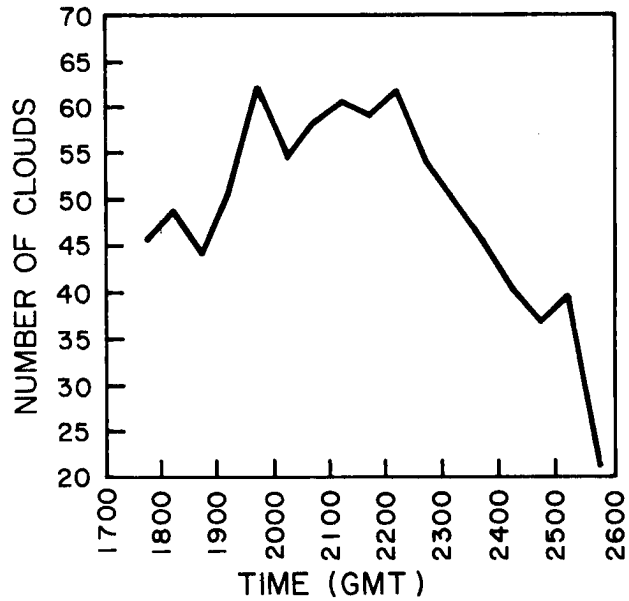


Fig. 42. Number of clouds (per observation) versus time of day for the northern high plains for 1976 (from Reynolds and Vonder Haar, 1978)

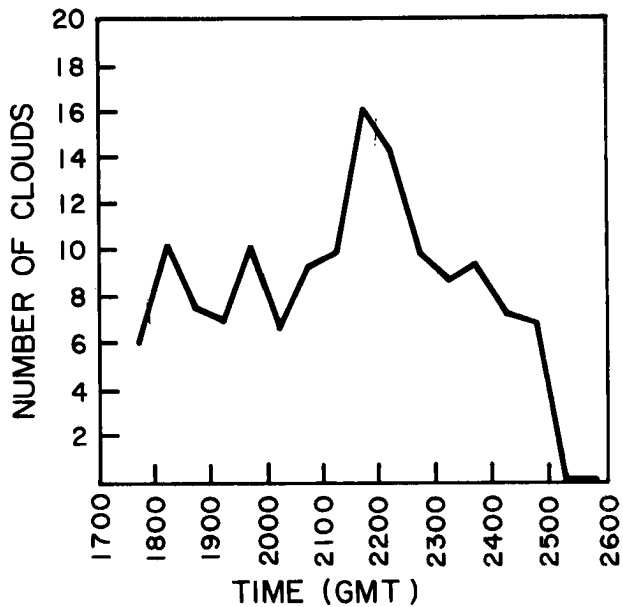
TIME VS NUMBER OF CLOUDS -  
WITHIN 175 km OF MLS

Fig. 43. Number of clouds (per observation) versus time of day for the Miles City target region for 1976 (from Reynolds and Vonder Haar, 1978).

in the composites increase by an average of 15% for the visible and 50% for the infrared between 18 GMT and 22 GMT. Recall that Reynolds and Vonder Haar's second study covered the period from 24 May - 15 July for one year, whereas this composite study cover 1 June - 31 July for two years. Cloud number, as calculated by Reynolds and Vonder Haar, is not quite the same as cloud frequency measured by the composites. Yet, both results verify the tendency for general cloudiness to increase after initial development around 18 GMT.

Reynolds and Vonder Haar also noted the importance of the Absaroka and Big Horn ranges in generating cloudiness in 1976 that moves into the Miles City area. Their plots of the number of clouds versus direction with respect to Miles City show at least three-and-one-half times more clouds in the southwest quadrant than in any other when the entire region (which includes the Big Horn Mountains) is considered, but a preference for clouds to be located in the northeast quadrant when considering areas within 175 km of Miles City. Plots of average cloud frequency for the four quadrants in the quantitative composite analyses for 1979 and 1980 (Figs. 23-38) do not show a preference for clouds to form in the lower left quadrant, even though qualitative analysis verifies the influence of the Absarokas and Big Horns. In fact, quantitative analysis of the composite imagery seems to verify Reynolds and Vonder Haar's earlier results for 1972-1974 indicating the area southwest of Miles City may be the least preferred region for cloud formation. While this second cloud climatological study of the HIPLEX region for 1976 was thorough and carefully executed, one must recognize that it includes data from only one season and that the analysis period does not coincide exactly with that for the composites. Of course cloud number is not quite the same as

cloud frequency, and Reynolds and Vonder Haar grouped all times together in analyzing cloud distribution. These differences in the data sets and analysis methods may account for some of the differences between cloud distribution results of the two studies.

Stodt (1978) examined cumulus clouds over several regions along the High Plains and Rocky Mountains using visible Defense Meteorological Satellite Program (DMSP) photographs from summer 1974. These satellite photographs have a higher resolution than GOES imagery, but because the satellite is a polar orbiter, it covers the target region only twice a day, once shortly before local noon and again at about midnight. Consequently Stodt usually only had one image per day on which to base his climatology. He discarded imagery if no cumulus occurred in his target areas, and also if cirrus clouds were present that could obscure lower cumulus clouds. After eliminating this imagery, Stodt's sample size was greatly reduced. He had six June images, one July image, and five August images for his Miles City target region, a circular area about 111 km in diameter centered at Miles City.

His two target areas in the Colorado Rocky Mountains, South Park and the Upper Arkansas River Valley, had 20 and 18 images respectively, met his criteria in June. For each of these two regions in July, 9 images were retained for analysis and in August, 17 images from the South Park area and 19 images from the Upper Arkansas River Valley had unobscured convection by local noon. Thus, in 1974, significantly more days had cumulus develop by local noon over mountainous terrain than over the northern Great Plains.

For the six images in June 1974, Stodt found an overall average cumulus cloud cover of 15% for his Miles City target area, and 18%, 20%, 11%, and 12% cumulus cloud cover for the northwest, northeast, southwest, and south east quadrants, respectively. These figures are all generally

lower than the average cloud frequencies measured by the 18 GMT June visible composites (see Figs. 23 and 27). June cumulus cloud cover in the northern half of Stodt's Miles City target region was 50% greater than for the southern half. Similarly, the average cloud frequencies for the 18 GMT June 1980 visible composite are about 52% greater in the northern half of the 256 by 256 pixel box (Fig. 27). However in the 18 GMT June 1979 visible composite (Fig. 23), the average cloud frequencies in the southern quadrants are about 20% greater than those for the two northern quadrants. Reynolds and Vonder Haar's two studies showed a greater number of clouds north of Miles City, but their data base included a great deal of imagery after local noon. Cloud distribution results from Stodt's cumulus cloud climatology over the Miles City area are similar to those from Reynolds and Vonder Haar's two studies and also to those from the composites. Yet Stodt's cloud cover results could differ significantly from a composite of geostationary imagery because so many images were discarded. The similarities between the cloud distribution results of these studies are interesting but not conclusive, because each experiment was designed and conducted differently and each measured a different entity.

Results from the earlier cloud climatological studies of the Miles City HIPLEX region can be compared to the composite imagery. But because these experiments and the present study were not designed with the same purpose in mind, they do not measure the same thing and should not be expected to do so. When the 1979 and 1980 HIPLEX cloud climatologies are completed, direct comparisons with the composites will be more meaningful: the question of year-to-year variation between data sets will not exist. The 1979 and 1980 HIPLEX cloud climatologies will

employ the same techniques of the earlier Reynolds and Vonder Haar HIPLEX work. Thus they will not only bridge together the earlier and more recent cloud climatologies but will also allow further assessment of the role of digital satellite composites in cloud climatology studies.

## VI. SUMMARY AND CONCLUSIONS

### VI.A Qualitative Analysis

The composite digital satellite imagery showed a relatively high frequency of clouds originated over certain mountain ranges and elevated areas along the lee slopes of the Montana Rocky Mountains. Regions where topography apparently enhances convective development included the Absarokas, the Big Horns, the Big Snowy Mountains, the Bear Paw Mountains, the ridgy area south and southwest of Miles City, Montana, and the Canadian Rockies west of Calgary.

In addition to showing which mountains have the greatest tendency to induce convection, temporal variations in the composites showed diurnal, month-to-month, and year-to-year variability in cloud frequency, distribution, and location over the High Plains. The magnitudes of these temporal variations confirm that other meteorological factors such as moisture availability are often more crucial than topographic influences in initiating High Plains convection. While composite imagery may become a valuable new research tool, inferences from composite imagery should acknowledge that a few years is, climatologically, a relatively short sampling period.

### VI.B Quantitative Analysis

Scatter plots, diagrams, and correlation and regression analyses showed that cloud frequency, as indicated by the composite imagery, and surface elevation are not linearly correlated. While the composite

imagery qualitatively demonstrated the influence of certain topographic features on the initiation of convection on the High Plains, absence of a linear correlation between cloud frequency and surface elevation may indicate any or all of the following:

- a) The relationship between surface elevation and cloud frequency in midlatitudes is not linear. Clouds form when many meteorological conditions such as stability, moisture availability, and convergence are favorable. Many atmospheric processes are described with nonlinear models; absence of a linear correlation between surface elevation and cloud frequency does not necessarily mean no relationship exists.
- b) Surface elevation is not the crucial topographic factor that causes some mountains to favor convective development. Slope, aspect, or absence of other local peaks may show good correlation with cloud frequency.
- c) The mountains are not as crucial in the evolution of High Plains convection as many have supposed. Moisture advection, stability, and mesoscale features may be more necessary than the lifting and convergence forced by the mountains.

Results from the composite imagery suggest that the mountains may help in initiating convection, but they are not the most important influence. After initial convective circulation begins (around or before 18 GMT), the initial topographic influences give way to mesoscale controlling features<sup>13</sup> that allow vigorous convection to take place almost anywhere along the High Plains.

---

<sup>13</sup>Such mesoscale features include "bubble" highs, meso-lows, downdrafts, and arc clouds.

### VI.C Conclusion

The composite imagery demonstrates the effect on convection of certain mountains and mountain ranges along the High Plains. Although for elevations above 1500 meters surface elevation and cloud frequency exhibited a weak positive correlation, surface elevation alone does not seem to determine which mountains are most effective in helping initiate convection -- probably eastern slope and aspect are more critical than surface elevation in determining which topographic features enhance convective development. Temporal variations of cloud frequency, distribution, and location suggest that the influence of topographic features on convection may be secondary to favorable moisture availability, stability, and convergence conditions. Stratifying the source imagery by environmental conditions (for example separating into a suppressed and an enhanced set) instead of by month may serve to show more of a mountain effect. Although developed for the purpose of demonstrating the relative influence of the mountains in initiating convection along the lee slopes of the Montana Rocky Mountains, the technique of compositing or averaging digital satellite data is a new research tool that will have many applications.

### VI.D Suggestions for Future Research

The addition of more powerful computing capabilities at Colorado State University's Direct Readout Satellite Earth Station will enable preprocessing of the source imagery to account for variations in radiance due to sun-earth-satellite geometry, if desired. In addition future compositing studies ought to include:

1. Determining the average visible radiance (with RMS average), average equivalent black body temperature of cloud-only cases,

and standard deviation of visible radiances and equivalent black body temperatures.

2. Stratifying the source imagery by synoptic situation, surface or mid-level winds, or other critical meteorological parameters (when sufficient imagery is available) to study how the atmosphere behaves in a certain situation; and grouping similar situations over different geographic areas (as long as topography is not a significant factor) after accounting for differences in ground albedo.
3. Conducting a study of weather radar data over the northern High Plains and comparing the results with this research.
4. Correlating monthly precipitation totals for reporting stations on the High Plains with visible and infrared composite imagery to determine the potential of using composites to infer rainfall.
5. Studying areas other than the High Plains to detect topography that influences convection or other atmospheric processes.

#### VI.E Potential Applications

While the technique of compositing digital satellite data was developed with the primary objective of determining the relative importance of topographic features in initiating High Plains convection, it has many potential applications. From a geostationary platform, remote areas where surface observations are sparse or infrequent can be monitored with regularity. With some adjustments, composite imagery could be used as proxy data to estimate precipitation or moisture variation over remote areas.

With the increased interest in climate changes and man's affect on climate, the archival of composited cloud frequency data would benefit climate monitoring and climate modelling efforts. Ellis noted in 1978 that climate study models could not adequately incorporate clouds and cloud effects in an iterative mode because of the lack of observational and diagnostic studies of cloudiness at the larger planetary scale.<sup>14</sup> Traditional surface observations of cloud type, amount of sky cover in tenths or oktas, and cloud base heights (usually estimated) were not sufficient to derive the quantities needed for energy transfer calculations (cloud top height and temperature, cloud absorptance, emittance, and reflectance). Ellis employed a 29 month composite of measurements from six satellites to quantitatively determine the effect of clouds on the planetary radiation exchange with space. Since then, much effort has been put into climate models. Henderson-Sellers et al. (1981) stressed the need for improved knowledge of cloud-climate variability for development of climate models. They recommended an intercomparing of satellite and surface cloud observations and also using satellite data to evaluate the frequency distribution of radiances above a cloud/no cloud threshold. Hence, the compositing technique developed here could help provide the necessary input for climate modelling in addition to facilitating the establishment of a more spatially continuous archive of cloud cover information.

Climatology is often used to predict what is most likely to occur based on what has happened in the past. Composites of satellite imagery could forecast the frequency, location, and distribution of cloud cover,

---

<sup>14</sup>Of course, the ADVISAR II allows analysis of digital satellite imagery on a variety of length scales, from meso to planetary.

as well as estimate the location and distribution of precipitation by proxy, provided the compositing covers a sufficiently long time period to be representative of the climatology.

Composite imagery can aid forecasters unfamiliar with local climatology, by showing where clouds will most likely form and how they will most likely progress. Being able to assess with satellite data how typical, with respect to local climatology, a synoptic or mesoscale situation is would alert forecasters to potentially difficult forecast situations.

With the increased capabilities of computers used for meteorological research, additional fields such as average albedo and average cloud top radiance, difference fields, found by subtracting one composite from another, and fields of statistics like the standard deviations of albedo and average equivalent black body temperature, will all be more feasible (economical) to compute. Correlation and regression schemes could be run on whole 512 by 512 pixel image arrays to analyze spatial, spectral, and temporal variations between composites. Addition of the VISSR<sup>15</sup> Atmospheric Sounder (VAS) to the geostationary satellites makes compositing of additional channels of moisture data possible. The ability of composite imagery to detect or verify a drought has been demonstrated. A cumulative composite image could be a useful tool in drought detection or verification, especially when additional moisture channels are routinely available. Compositing digital imagery could create a new climatological data base that could serve as input for general circulation models.

---

<sup>15</sup>Visible and Infrared Spin Scan Radiometer.

## BIBLIOGRAPHY

- Arnold, C. P., 1977: Tropical Cyclone Cloud and Intensity Relationships. Atmospheric Science Paper 277, Colorado State University, Fort Collins, CO, 154 pp.
- Dirks, R. A., 1969: A Theoretical Investigation of Convective Patterns in the Lee of the Colorado Rockies. Atmospheric Science Paper 154, Colorado State University, Fort Collins, CO, 222 pp.
- Ellis, J. S., 1978: Cloudiness, the Planetary Radiation Budget, and Climate. Ph.D. Dissertation, Colorado State University, Fort Collins, CO, 129 pp.
- Elterman, L. and R. B. Toolin, 1965: Atmospheric Optics. In Handbook of Geophysics and Space Environments. Air Force Cambridge Research Labs., Cambridge, MA, CW7, 36 p.
- Grant, L. O., G. W. Brier, and P. W. Miekle, Jr., 1974: Cloud Seeding Effectiveness of Augmenting Precipitation from Continental Convective Clouds. Proceedings of the International Tropical Meteorological Meeting, 31 January - 6 February 1974, AMX, Nairobi, Kenya, 5 pp.
- Griffith, C. G., J. A. Augustine, and W. L. Woodley, 1981: Satellite Rain Estimation in the U.S. High Plains. J. Appl. Meteor., 20, January, 53-66.
- \_\_\_\_\_ and W. L. Woodley, 1973: On the Variation with Height of the Top Brightness of Precipitating Convective Clouds. J. Appl. Meteor., 12, September, 1086-1089.
- \_\_\_\_\_, W. L. Woodley, P. G. Grude, D. W. Martin, J. Stout, and N. Sikdar, 1978: Rain Estimation from Geosynchronous Satellite Imagery -- Visible and Infrared Studies. Monthly Weather Review, 106, August, 1153-1171.
- Henderson-Sellers, A., N. A. Hughes, and M. Wilson, 1981: Cloud Cover Archiving On A Global Scale: A Discussion of Principles. Bull. Amer. Meteor. Soc., 62, September, 1300-1307.
- Henz, J. F., 1973: Characteristics of Severe Convective Storms on Colorado's High Plains. Preprints Eighth Conference on Severe Local Storms, October 15-17, American Meteorological Society, Denver, CO, 8 pp.
- \_\_\_\_\_, 1974: Colorado High Plains Thunderstorm Systems: A Descriptive Radar -- Synoptic Climatology. Master's Thesis, Colorado State University, Fort Collins, CO, 82 pp.

- Klitch, M. A., 1981: Some Suspected Regions of Enhanced Convective Development Along the Montana Rocky Mountains. (Unpublished) 15 pp.
- \_\_\_\_\_, 1982: Compositing GOES Data to Detect Regions of Enhanced Convective Development Around Eastern Montana. Master's Thesis, Colorado State University, Fort Collins, CO, 95 pp.
- Kornfield, J. and A. F. Hasler, 1969: A Photographic Summary of the Earth's Cloud Cover for the Year 1967. J. Appl. Meteor., 8, August, 687-700.
- Maddox, R. A., 1980: Mesoscale Convective Complexes, Bull. Amer. Meteor. Soc., 61, November, 1374-1387.
- \_\_\_\_\_, 1981: The Structure and Life-Cycle of Midlatitude Mesoscale Convective Complexes. Atmospheric Science Paper 336, Colorado State University, Fort Collins, CO, 311 pp.
- McCartney, E. J., 1976: Optics of the Atmosphere; Scattering by Molecules and Particles. Chapter 4 -- Rayleigh Scattering by Molecules. John Wiley and Sons, New York, pp. 176-215.
- Miller, R. C., 1972: Notes on Analysis and Severe-Storm Forecasting Procedures of the Air Force Global Weather Central. Air Weather Service (MAC), United States Air Force Technical Report 200 (Rev.).
- Oliver, V. J. and R. A. Scofield, 1976: Estimation of Rainfall from Satellite Imagery. Sixth Conference on Weather Forecasting and Analysis, 10-13 May 1976, Albany, NY (AMS, Boston, MA).
- Phillips, C. B., 1979: Observation of Progressive Convective Interactions from the Rocky Mountain Slopes to the Plains. Atmospheric Science Paper 316, Colorado State University, Fort Collins, CO, 100 pp.
- Reynolds, D. W. and T. H. Vonder Haar, 1973: A Comparison of Radar-Determined Cloud Height and Reflected Solar Radiance Measured from the Geosynchronous Satellite ATS-3. J. Appl. Meteor., 12, September, 1082-1085.
- \_\_\_\_\_ and \_\_\_\_\_, 1975: Satellite Support to the HIPLEX Activities for 1975. Department of Atmospheric Science, Colorado State University, Fort Collins, CO, Final Report, Bureau of Reclamation, Contract #14-06-D-7630. 137 pp.
- \_\_\_\_\_, 1978: Satellite Support to the HIPLEX Activities for 1977. Department of Atmospheric Science, Colorado State University, Fort Collins, CO, Annual Report, Bureau of Reclamation, Contract #6-07-DR-20020.

Scofield, R. A. and V. J. Oliver, 1977: Using Satellite Imagery to Estimate Rainfall from Two Types of Convective Systems. Eleventh Technical Conference on Hurricanes and Tropical Meteorology. 13-16 December, 1977, Miami Beach, FL (AMS, Boston, MA).

\_\_\_\_\_ and \_\_\_\_\_, 1980: Some Improvements to the Scofield/Oliver Technique. Second Conference on Flash Floods, 18-20 March 1980, Atlanta, GA (AMS, Boston, MA).

Sellers, W. D., 1965: Physical Climatology. University of Chicago Press, Chicago, IL, 272 pp.

Smith, E. A. and T. H. Vonder Haar, 1980: A First Look at the Summer MONEX GOES Satellite Data. Fifteenth AIAA Thermophysics Conference, July 14-16, 1980, Snowmass, CO, 16 pp.

Stodt, R. W., 1978: Summertime Satellite Cumulus Cloud Climatology. Master's Thesis, Colorado State University, Fort Collins, CO, 92 pp.

Trewartha, G. T., 1968: An Introduction to Climate. McGraw-Hill Book Company, New York, NY, 408 pp.

## APPENDIX

### SOURCES OF ERROR

In general, three kinds of errors could occur in this experiment: those attributable to errors in measurement, to errors in interpretation of the data, and to errors in inferences one might make from the results.

Measurement errors can arise from problems with the satellite's radiometers or in their calibration and from the variations of the sun-earth-satellite geometry that cause variations in the detected radiation that are separable from radiance variations with meteorological significance. The cloud/no cloud decision arbitrarily applied by the compositing algorithm, solely on the basis of digital satellite counts, could be in error because the cloud threshold theoretically should be slightly different for each pixel because the incident solar radiation, which has a large affect on how bright clouds appear to the satellite, varies with latitude, time of day, and time of year. Also, incoming and outgoing radiation is filtered somewhat by the earth's atmosphere; the more atmosphere the radiation must travel through, the more attenuation from the atmospheric constituents it will experience. The variations in sun-earth-satellite geometry which affect the radiation over the region were considered small enough to ignore in this analysis. In general the geometry does not change significantly over a month's time to bias a composite image. The diurnal variation of brightness was accounted for by using a lower cloud threshold for the 22 GMT visible imagery. The

variation of radiance due to solar zenith angle and satellite zenith angle variations over the displayed image was not significant enough to merit incorporating these variations into a preprocessing normalization scheme.

Parallax error is another type of measurement error. It is defined as the error incurred when extrapolating a cloud's position to the earth's surface instead of to a point above the earth. Parallax error depends on two factors: the satellite zenith angle and cloud height. The further away a cloud is from the satellite subpoint, the greater the satellite zenith angle, and the greater the parallax error. The higher a cloud is, the greater the difference between its actual location and that inferred from extrapolating its position to the earth's surface. Over a month's time the range of cloud heights at any given location varies. For the no cloud case, there is no offset due to parallax error. For low cloud tops of 3000 meters the parallax offset would be 2.5 pixels or about 5.7 km to the northwest. And for a well-developed towering cumulus with a top of 12,000 meters the parallax offset would be 10 pixels or 22.8 km to the northwest. Given that the composite imagery is employed to detect regions where topography enhances convective development that may be 200 square km in extent, the significance of parallax error in this analysis is relatively small.

Many sorts of interpretive errors could occur so it should be stressed that the composite imagery depicts cloud frequencies, based on a pixel's digital count is above a specified cloud threshold. A composite image may appear to be an average satellite picture, but it is not.

When the satellite scans the earth, the radiances it senses are digitized into counts from 0 to 63 for visible wavelengths and 0-255 for the infrared. To make best use of the dynamic range, the transfer

function for relating visible radiances to digital satellite counts is such that the visible count squared is proportional to radiance (Smith, 1980). An average visible radiance cannot be inferred from the visible composite imagery shown in this paper. Although the transfer function for converting infrared digital counts to infrared radiances is basically linear, neither an average infrared radiance nor an average equivalent black body temperature can be inferred from the infrared cloud frequencies in the composites. While depicting the average visible or infrared radiance and the average equivalent black body temperature would be interesting to many scientists, this was not done in this study because the extra computations required would be no improvement over a simple cloud frequency algorithm in identifying areas where topographic features enhance the development of convective clouds. Such computations, however, could be added in future compositing studies to shed new light on High Plains convection and complement radiation budget research.

Despite the relatively constant input that controls the weather -- the solar constant, land-sea distribution, topography, and ground albedo -- weather changes can occur with such capriciousness that any weather statistics, especially averages, ought to be treated with care. These composite images represent averages of a sort, and while valuable information may be gleaned from them, inferences from composite imagery must be cognizant of limitations of the data.

These composites cover only two summers. Over these two seasons, significant variations in the location, frequency, and distribution of cloudiness were observed and interpreted with current theories on the evolution of High Plains convection and available weather data. While the drought of 1980 was considered an anomaly, weather commonly is

expected to deviate from the normal. Climatological averages are usually derived from continuous records covering over 30 years. Geostationary satellites have not been operationally observing the atmosphere for nearly that long. Climatological tendencies, therefore, should not be inferred from the composite imagery without guarded reservations.

Also, logistics prevented every day in the sampling period from being available. Composites in this study were made from 18 to 23 days of a possible 30 or 31 in a month. The necessary omission of unavailable data implies the possibility of bias -- if the missing days in a month were significantly different from those that comprised the composite, generalizations about the cloud frequency, distribution, and location based on the composite imagery, would be in error. Since the missing days were mostly due to equipment failure and lack of Sunday data collection, their occurrence was basically random and the likelihood that their omission would bias the composite is small.

Due to the randomness of the occurrence and type of different synoptic events (fronts, dry lines, etc.), composites can vary from month-to-month or year-to-year and still be well within the realm of normal. To eliminate this potential bias from compositing, stratifying the source imagery by synoptic situation was suggested. This would eliminate the smoothing that results from averaging all images and probably would highlight the crucial features in a synoptic situation that could ultimately be useful to a forecaster. Imagery was not stratified by synoptic situation in this study because there was not

enough data to produce statistically significant results.<sup>1</sup> Future compositing studies, utilizing a larger data base, may take this approach.

In drawing conclusions from the data presented in these composite images, one must be aware of the sources of error involved in the measurements, computations and related assumptions that have taken place. Potential errors in interpreting these data have been outlined above. While the technique of compositing digital satellite data can have many predictive applications, care should be exercised when inferences are made from composite imagery.

---

<sup>1</sup>Henz documented eleven potential severe weather patterns which occur along the High Plains (Henz, 1973). Assuming there are also several fair weather patterns, and recognizing that some of the satellite data over the two month period were not available, perhaps an average of six cases of each synoptic situation might occur during the two years.